Scholars' Mine

Masters Theses   Student Theses and Dissertations

Spring 2015

EMI analysis of DVI link connectors

Abhishek Patnaik

Follow this and additional works at: https://scholarsmine.mst.edu/masters_theses

Part of the Electromagnetics and Photonics Commons

Department:

Recommended Citation

EMI ANALYSIS OF DVI LINK CONNECTORS

by

ABHISHEK PATNAIK

A THESIS

Presented to the Faculty of the Graduate School of the

MISSOURI UNIVERSITY OF SCIENCE AND TECHNOLOGY

In Partial Fulfillment of the Requirements for the Degree

MASTER OF SCIENCE IN ELECTRICAL ENGINEERING

2015

Approved by

Dr. David Pommerenke, Advisor
Dr. James Drewniak
Dr. Jun Fan

ABSTRACT

EMI problems are not uncommon in high speed communication systems. As the system clock frequencies increases, so does the challenges in controlling the EMI in such systems. A connector is a very important part of a high speed communication system. Electromagnetic interference (EMI) is found to be tightly correlated to mode conversion: from differential-mode (DM) signals to common-mode (CM) currents and further to antenna-mode (AM) currents on the outside of cables or enclosures. Moreover, in such high speed systems, coupling to an adjacent cable-connector system is not uncommon. It is essential to understand and quantify this coupling path in order to mitigate the coupling. Though simulation based methods are widely used, such an approach is generally very time consuming and computationally resource hungry and an effort is made to quantify the coupling paths using measurement-simulation combinations with minimal simulation aid. This thesis presents a systematic approach to isolate and identify the different coupling paths in a high speed interface (in this case we show DVI), as well as identify which discontinuity (and hence the coupling path) is most critical to mitigate EMI. A transfer function based method is implemented to quantify the coupling in the connector cable system. The method developed in this study can be used for any high-speed interface in modern communication systems.

ACKNOWLEDGMENTS

I would like to express my gratitude to all those who have helped me during this research. Firstly, I would like to thank my advisor Dr. David Pommerenke for giving me the opportunity to work on this project, his valuable insights and suggestions have helped me to overcome many hurdles during this work. I am grateful to him for the advice and guidance he gave me throughout my Masters program. I also thank Dr. Pommerenke for his moral support during my tough times by understanding and encouraging me to focus on my goals. I would like to thank Dr. Drewniak and Dr. Fan for being part of my thesis committee and taking time to review this work.

I would like to thank Dr. YaoJiang Zhang at Missouri University of Science and Technology and Chen Wang and Chuck Jackson at NVIDIA, Inc. for their assistance during the course of this thesis and also for providing the hardware which served as a research subject during this entire thesis study.

A special thanks to all my friends whose constant support and encouragement has always been crucial for me. Finally, I would like to dedicate this work to my parents (Biswajit and Seema) for their emotional support and unconditional love and sacrifices.

TABLE OF CONTENTS

Page

LIST OF ILLUSTRATIONS

LIST OF TABLES

1. INTRODUCTION

The digital visual interface (DVI) connector is partially inside and partially outside the computer chassis or enclosure. DVI uses a high-speed serial link called transition minimized differential signaling (TMDS) to transmit signals between the CPU and the monitor using a DVI cable [1]. Although differential signals cause weak radiations, it can be converted to common-mode (CM) currents and further to antenna-mode (AM) currents flowing on the outside of the chassis and the DVI cable [2],[3],[4].

Figure 1.1 shows some of the discontinuities in the DVI signal link. The discontinuities such as the connector body shell gaps, gaps between the connector shell and the DVI cable shell as well as the gaps between the connector and the CPU enclosure are the main reasons causing this mode conversion [5].

According to the equivalent principle, the voltages along these gaps can be regarded as secondary radiation sources causing the cable and the enclosure to radiate. This implies that the connector imperfections can work as feeding sources while the DVI cable and enclosure are the antenna structures [6]. In a DVI interface, the connector forms an important link between the source and the receiver system connected by the DVI cable. The connector is housed in a back shell also referred to as the connector shell or shield (Figure 1.1). The main purpose of the connector shell is to provide a continuous closed conductive envelope in order to prevent outside fields from penetrating and internally generated noise from emerging out. Ideally this shield should make a 360° direct electrical contact with the outer supporting metallic bracket enclosure system [5],[7]. However, it is very difficult to obtain such a perfect shield from a manufacturing and assembly point of view. Therefore, the connector body shell has certain apertures as well as non-uniform contact points with the
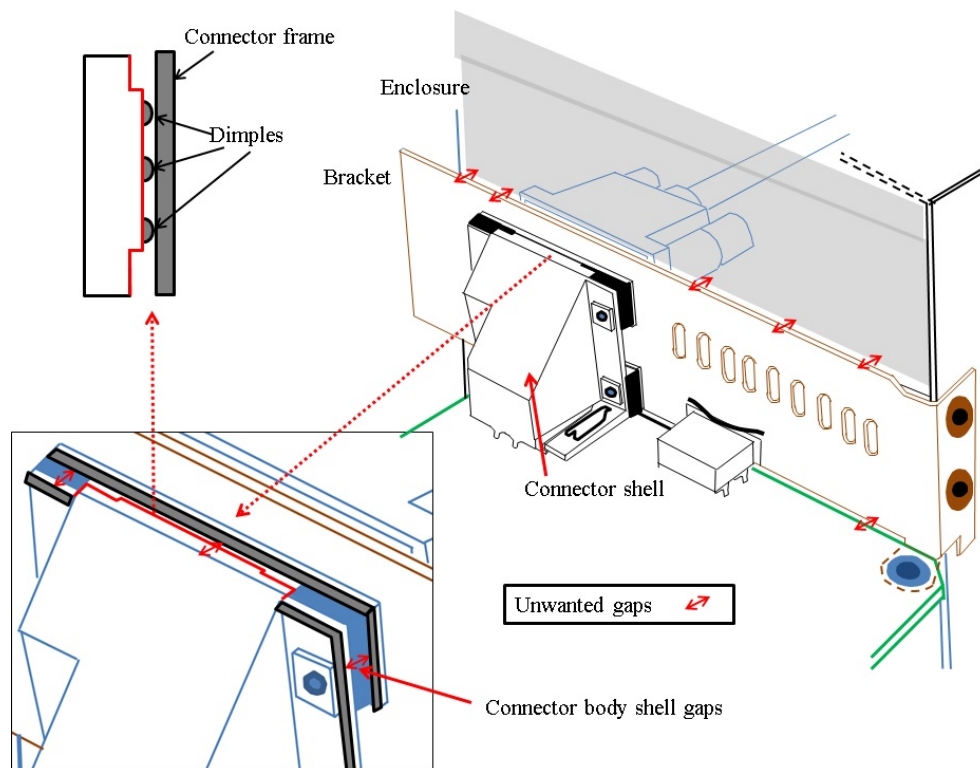
Figure 1.1. Different gaps in a DVI connector link

bracket. Each aperture reduces the shielding efficiency of this shield that results in increased susceptibility and emissions as electromagnetic energy can leak through these apertures. Many studies have shown how the apertures on the shield of a high-speed connector can hamper the shielding effectiveness of a connector [8],[9],[10],[11],[12]. It is important to ensure that no aperture on the connector body shell approaches $\lambda/2$ in length since that would cause the aperture to turn into a good energy radiator and cause severe EMC issues [5]. It has been studied that the connector shell continuity should also be extended to the enclosure of the entire system while maintaining low impedance between the other critical contacts such as the connector-shell and cable-shell assembly [13],[14]. In general, a very well shielded cable connected to a connector having a poor shielding effectiveness would render the entire systems EMI performance to drop significantly. But there are situations where a connector with

apertures would still perform well. It might be acceptable to have a connector body shell with apertures as long as the enclosure to which the connector is mounted on is completely shielded and has no slots/apertures/seams. At the same time the contact between the connector frame and the enclosure along with the bracket has to be complete and circumferential. In this case the cable-shell to connector-shell contact has to be circumferential 360° for an effective shielding regardless of the connectors shielding inside.

A slight deviation from the above ideal case can degrade the overall EMI performance of the system no matter how good the connector shield/cable shield is. But such is not the case with actual systems. In an actual enclosure system there are many slots/apertures/seams for multiple reasons such as cable routing, ventilation, mechanical contacts, acoustics etc. The amount of leakage from the aperture depends mainly on the linear dimension, the wave impedance and the frequency of the signal. Moreover, more the current has to detour, more the shielding is reduced [15]. These crucial contacts in the connector-enclosure-cable system can be represented as equivalent inductances [12]. Looking at these contacts from the perspective of return current path gives a better insight as why they can be regarded as equivalent inductances. Suppose a good circumferential connection is made between an interconnect, then the return current would flow without any obstruction, but once the contacts are restricted to tap points or dimples as in the case of the connector shell-cable shell contact, the current now constricts and has to flow through these dimples (Figure 1.2). We know when the flow of current is impeded by these geometrical structures (dimples), it can be regarded as an equivalent inductance.

Understanding the imperfections in the return path of currents is important in order to mitigate EMI problems. The best solution is to have a good layout design at the design phase taking into consideration all the good design practices and have provisions for additional filtering on most of the high speed signal lines where
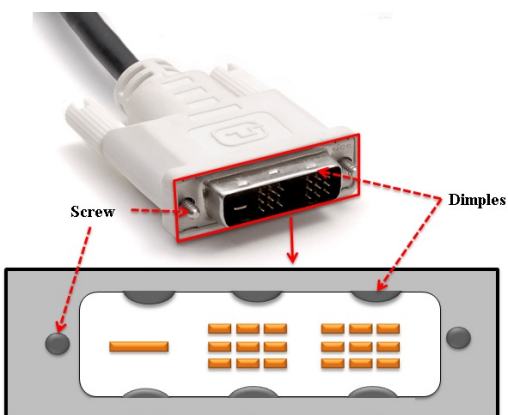
Figure 1.2. Illustration of dimples on a cable connector

possible. High-speed signal lines should not have many transition vias as this may further excite the power-GND planes through which it penetrates and further increase the EMI issues. Following similar good design practices prevent the risk of having to re-manufacture the board during the debug phase of a product when it fails the EMI compliance testing. Not only will a re-manufacture add to an overhead cost to the entire project budget but also impacts the final shipment of the product that can further add to the losses incurred by the company.

1.1. MOTIVATION

When good design practices are followed and the end design still fails the strict compliance testing requirements, sometimes it can be attributed to the connectors and cables routing within the system which act as excitation sources or antennas in a typical system allowing the internal energy from within the system to leak out into its surroundings through some coupling path. Having a good understanding of such coupling paths, design improvements for connectors and additional components and even layout changes can be suggested to so as to improve the overall EMI performance.

Simulation methods are sometimes effective in-order to estimate the EMI performance. A major downside of simulating the entire system is the computation size and resources necessary. For a complex system, of cables, connectors and boards, it may be necessary to model every detail in-order to capture its actual impact. This would make the simulations extremely large, resource hungry and time consuming. It would be interesting to be able to identify the different coupling paths and simulate the system by making changes to the important structures associated with the coupling paths to see the reduction in the EMI, however additional time and resources may be necessary if the impact of each and every detail is necessary to be studied. A study to be able to quantify the coupling paths in such a system without using a complete simulation model is quite beneficial. Being able to understand these coupling paths makes it easier to debug the EMI issues in such a cable-connector system. Hence a method where the impact of certain design changes can be studied without the use of heavy computational resources is investigated which can help in making quick engineering judgments has been developed.

1.2. ORGANIZATION OF THESIS

This thesis is presented in order to study the various important contacts/ imperfections in the DVI signal link by identifying the mode-conversion mechanisms and quantifying the impact of the imperfections in the DVI signal link towards EMI due to the AM currents. The EMI problem associated with a high-speed connector cable system link is analyzed by breaking the entire signal path into different blocks and quantifying the impact of each block towards the overall EMI performance. The impact of each block has been quantified in the radiated field. The system is divided into different blocks such as:

1. The connector itself

2. The connector-cable assembly

- The cable itself

- The connector-cable system

3. Adjacent connectors

While some parts are quantified based on simple mode conversion and gap voltage generation, a detailed study has been presented on the connector-cable assembly with the derivation of a transfer function to quantify the mode conversion and evaluate the impact of the major imperfections at this interface. The underlying idea is to be able to identify and quantify the different coupling paths as well as identify the important contributing imperfections in the DVI signal path that would have the most impact on the EMI performance of the entire system. After identifying this important imperfection, it would make it easier in suggesting design changes that would be most beneficial in reducing the EMI of the system. The rest of this thesis is organized as follows. In Section 2, a background related to the different currents and the EMI problem related to a DVI system is illustrated. Section 3 explains coupling paths in such high speed connectors illustrated on a DVI system. Further section 4 deals with the methods used to quantify the mode conversion in the connector, the connector cable assembly and coupling to adjacent connectors. For the connector, the mode conversion at the major slots on the connector body and the coupling path related to it are identified after which the dominating slot is determined and its effect is verified in the standard radiated field tests. For the mode conversion in the connector cable assembly a test setup is designed to identify the important interfaces and derive a transfer function to predict the radiated field that is validated with the measurements. The coupling to adjacent connectors is studied based on a combination of measurement and simulation methods.

2. BACKGROUND

This chapter focusses on explaining the different types of currents on a cable and has been extended to a high speed DVI connector cable system.

2.1. TYPES OF CURRENTS

The DVI signal driver may send both differential-mode (DM) and common-mode (CM) currents. The DM currents may give rise to CM currents when it encounters discontinuities along its path like traces, DVI connector, load end terminations, etc. Usually there are both DM and CM currents flowing along the differential pair signal lines. The CM return currents would flow through the inner surface of the shielding braid. However, if there is a discontinuity along the braid, the CM return currents will flow along the outer surface of the braid(the least impedance path). Different modes of current are illustrated in Figure 2.1.
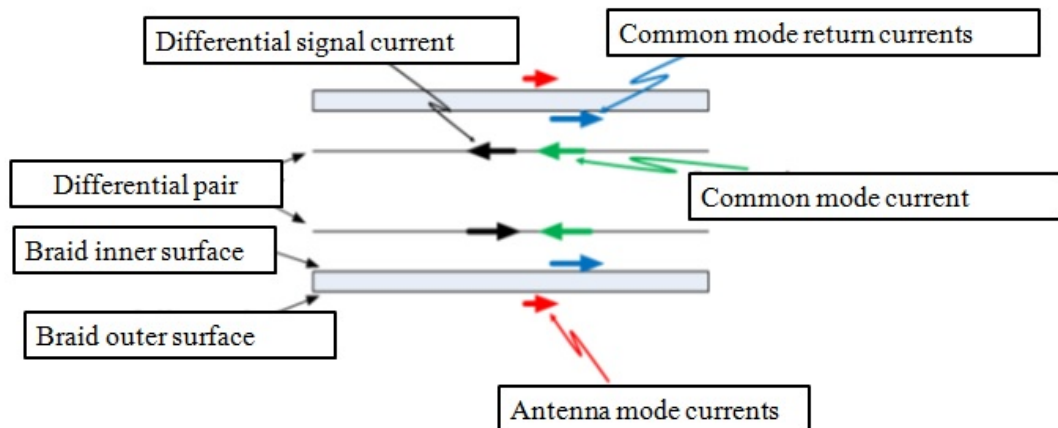

Figure 2.1. Different currents on a cable

We define antenna mode (AM) currents as those currents that flow on the outside of larger metal parts, such that they cause EMI. The term antenna mode currents is selected to distinguish between the CM currents that do not cause EMI (e.g., the CM current inside the shielded cable), and the CM currents that cause EMI (e.g., the fraction of the CM current that flows on the outside of a shielded cable). This AM current will act as feeding sources to excite the surrounding structures and cause EMI problems.

To investigate the mode-conversion in a more complex DVI signal link, let us assume an ideal differential signal flowing along a differential pair Tx- and Tx+ as shown in Figure 2.2. Part of the DM currents would get converted to CM currents due to the discontinuities of pins and asymmetric geometry of Tx- and Tx+ with reference to the GND pins and the connector cover. The CM return current will flow through the GND pins of the connector, the inner side of the shield of the connector, and the inner surface of the shield of the DVI cable as shown in Figure 2.2. The blue arrows on the DVI cable represent the CM return currents on the inside of the cable. They return to the DVI cable shell and connector shell through six tiny contacts or dimples which connect with the connector shell represented by inductances as shown in Figure 2.2-A, wherein the inductances between the connector shell and the cable shell are used to symbolize the connector shell- cable shell gap. The induced voltages along this gap will excite AM currents on outer surfaces of the cable and the chassis. In addition, when the return currents encounter the gap between the shell-bracket (Figure 2.2-B) or bracket-enclosure (Figure 2.2-C), similar gap voltages can also be induced and AM currents are further excited on the surfaces of the connector outer shell and chassis.
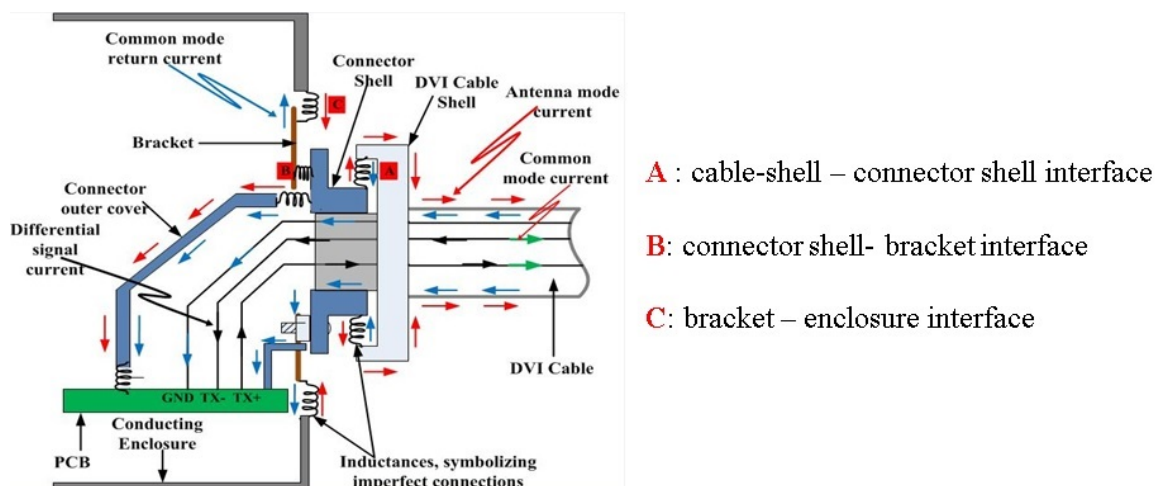
Figure 2.2. Current flow in a DVI connector- cable system

2.2. EMI TESTS ON A DVI CONNECTOR SYSTEM

An actual computer system with a graphics card having a dual stack DVI connector connected to a LCD display was selected as our research target. To identify the EMI problem, the computer system was placed inside a semi anechoic chamber with the display being driven by the top DVI connector. The standard 3m FCC radiated field test performed on the system shows the harmonics of the DVI spectrum in the radiated field test (Figure 2.3) that can cause the product (graphics card) to fail EMC certifications.

A first level check is to identify the major antenna structure in the system. In this frequency range, the DVI cable can by itself form an effective antenna [3]. With the AM current on the DVI cable having a DVI CM spectrum signature, it radiates quite effectively showing the harmonics of the DVI clock in the radiated field tests (Figure 2.3, 2.4). For a given display resolution, the critical clock harmonics of 445.5MHz and 742.5MHz strongly show up in the radiated field tests with the 5th harmonic (742.5MHz) only a few dB lower than the FCC class B limit (Figure 2.4).
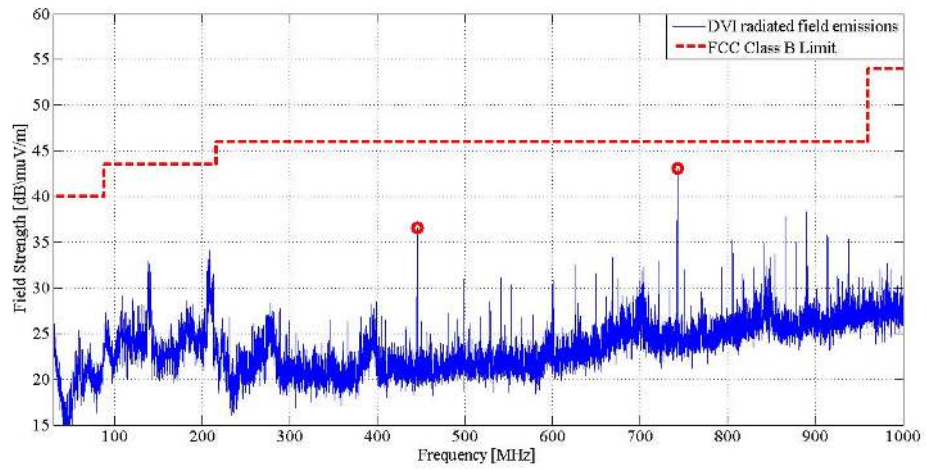
Figure 2.3. Field strength measured at 3m for the DVI system

Figure 2.4. DVI clock harmonic at 742.5MHz

3. DVI LINK COUPLING PATH ANALYSIS

There are many interfaces in the DVI link system. The mode conversion from some of the interfaces has been identified and the coupling paths are presented in this chapter. The coupling paths have been illustrated in the form of a coupling path diagram as in Figure 3.1 and later explained.

Figure 3.1. Coupling paths
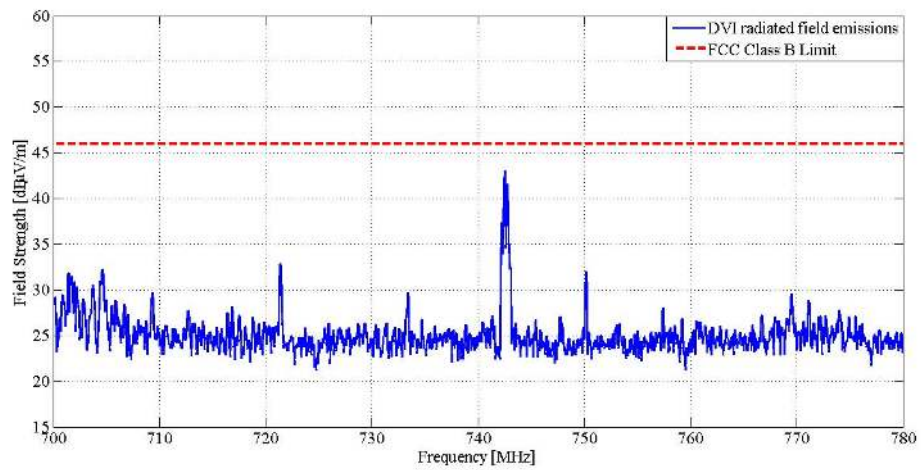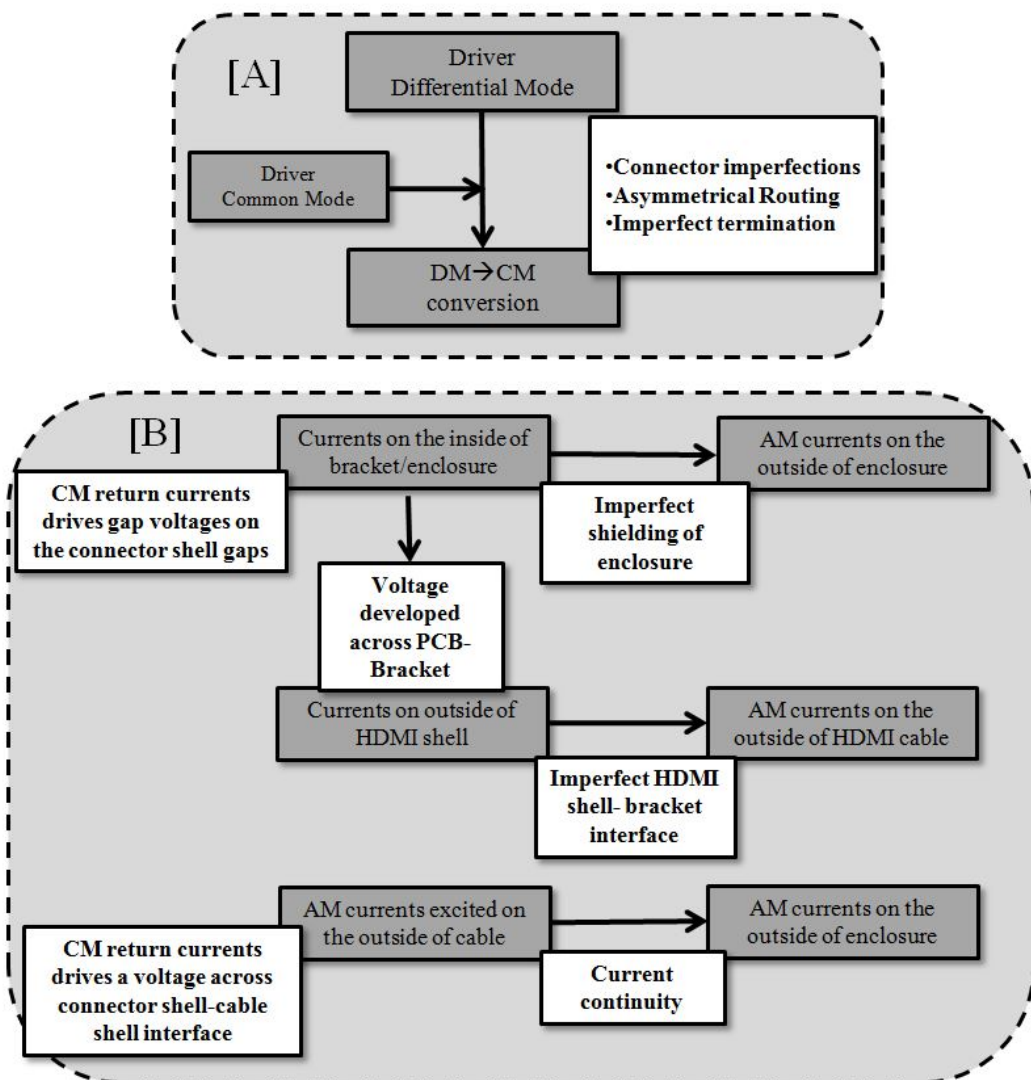
Aiming at a segmented model, the first step is dividing the complex problem into blocks that are easier to understand and the second step is to quantify each block. This can help towards the improvement of the overall design and introduce a more systematic approach of understanding the EMI in the DVI system thus providing a good tool for engineering judgment. Based on the radiation of the DVI system, the electromagnetic coupling paths and mechanisms from the driver signal to the AM currents have been qualitatively understood and identified. The path includes the graphics card PCB, DVI connector, chassis, and the DVI and HDMI cables. The coupling path diagram shown in Figure 3.1 identifies the major mode conversions in the DVI connector link. Figure 3.1-A represents the mode conversion from DM from the driver to CM in the signal link. The CM current can be caused by asymmetry in the driver, the PCB layout design, the connector, the cable connector, cable asymmetry, the receiver side termination, etc. In fact the driver may itself drive a signal with some inherent CM. Figure 3.1-B focuses on the connector-cable structures and the coupling paths associated with them. Three important coupling paths are described with illustrative figures in the following sections. These coupling paths have later been quantified using measurement and simulation based techniques.

3.1. COUPLING PATH 1 - CONNECTOR BODY IMPERFECTIONS

As in most connector body shell assemblies, the dual stack DVI connector has many body shell gaps or apertures that make contact at intervals along its length and sides (Figure 3.2). The gaps in the connector form a main coupling step to excite nearby structures. For example the seam between the top flange of the connector shell and the connector frame (Figure 3.2-D) makes contact to the body frame by three tiny dimple like structures. For this seam an equivalent inductance can be expressed as the current is impeded to flow through only these dimples. Often these
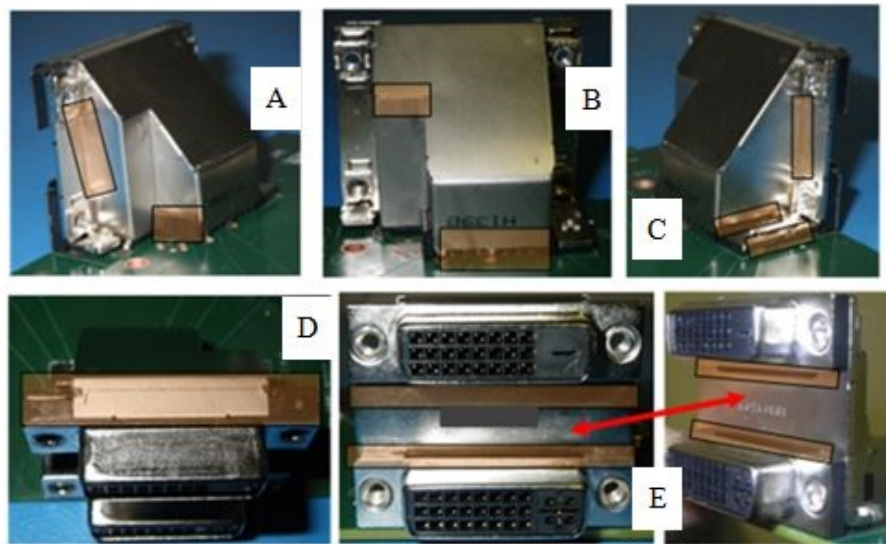
Figure 3.2. Connector body shell gaps

seams offer high rf impedance, but contacts (dimples) at intervals along the length of the seam can parallel the inductance of the connections thus reducing the equivalent impedance. Such inductances will have a voltage drop across it due to the CM return currents, which in turn will act as a source to drive antenna mode currents on the outside metallic structures, like on the bracket, the enclosure body, DVI cable, etc. thus causing them to radiate. Figure 3.3 shows a visual interpretation of the currents and the gap voltages which further drive AM currents on the inside of the bracket-enclosure and due to imperfect shielding of the enclosure, antenna mode currents flow on the outside of the enclosure and cable shield.

3.2. COUPLING PATH 2 - CONNECTOR - CABLE ASSEMBLY

This coupling path deals with the coupling related to the connector cable assembly structures which involve the connector, bracket, enclosure and cables. The

CM return current drives gap voltages across the black plastic parts of the connector

CM return currents on inside shell

CM return current

Displacement current

Voltage developed between surfaces

The developed voltage drives currents on the inside of the bracket/Enclosure.

Due to Imperfect shielding of the enclosure antenna mode current is on the outside of the enclosure.

Figure 3.3. Mode conversion from the connector body shell

coupling path illustrated in Figure 3.4 explains the coupling path through the connector shell-cable shell mating interface. The connector shell-cable shell interface can drive antenna mode currents on the cable and enclosure as well. With a well shielded cable and connector, the interface at this shell-shell interface is still very important towards the overall EMI performance of the system. An imperfect contact at this interface will have a connector shell-cable shell voltage developed which in turn can drive antenna mode currents on the outside of the cable and enclosure system. This interface along with other interfaces such as the shell-bracket, bracket-enclosure are illustrated with inductances in Figure 3.4 in side view.

The shell to shell voltage drives a current on the cable outside, so causes an antenna mode. This current, because of current continuity also flows on the outside of the enclosure

DVI cable

Enclosure

Bracket

PCB
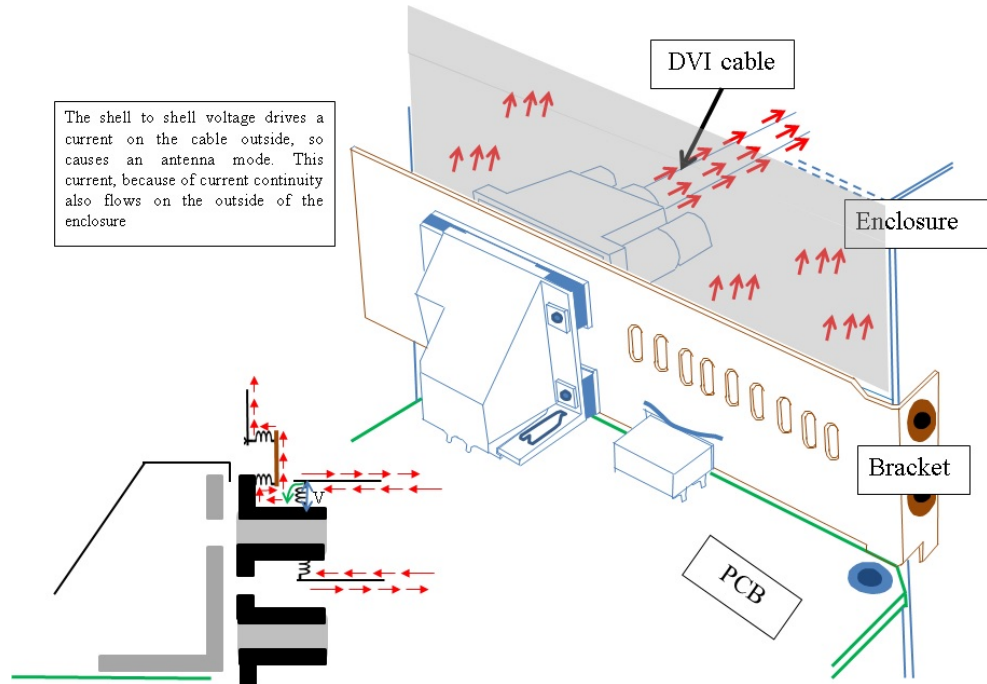
Figure 3.4. Mode conversion in connector shell-cable shell interface

3.3. COUPLING PATH 3 - COUPLING TO ADJACENT CONNECTORS

The coupling to adjacent connectors has been studied here taking an example of a HDMI connector mounted on the same PCB sharing the enclosure mounting bracket with the DVI connector. The next assumption is that there is no coupling from the outside of the enclosure, ex. from the DVI cable to the HDMI cable. Here the coupling from a DVI connector to a HDMI connector-cable system results in AM current on the HDMI cable having the DVI CM spectral content. The coupling to the adjacent HDMI connector is mainly caused due the DVI link system via two coupling mechanisms. Firstly, the coupling may occur inside the PCB, e.g. the DVI signals can excite a power ground plane cavity which propagates the signal to the HDMI signal at a HDMI via transition through power ground plane. This would lead to the DVI's spectral content becoming visible on the HDMI signal, but not necessarily

as AM on the HDMI cable having the DVI spectral content. The second coupling path is outside the PCB, but inside the enclosure and is caused by the imperfect shielding of the DVI connector and imperfect contact of the HDMI connector shell taps to the bracket (Figure 3.5). Here the connector gap voltages driven by the CM return currents can drive currents on the inside of the bracket and PCB. The voltage developed across the PCB-Bracket drives a current on the HDMI connector shell. An imperfect contact at the HDMI shell-bracket interface drives the DVI common mode spectral content AM current on the outside of the HDMI cable. Both of the above coupling paths have been studied in more detail in subsequent chapters and the most dominating coupling path has been quantified.
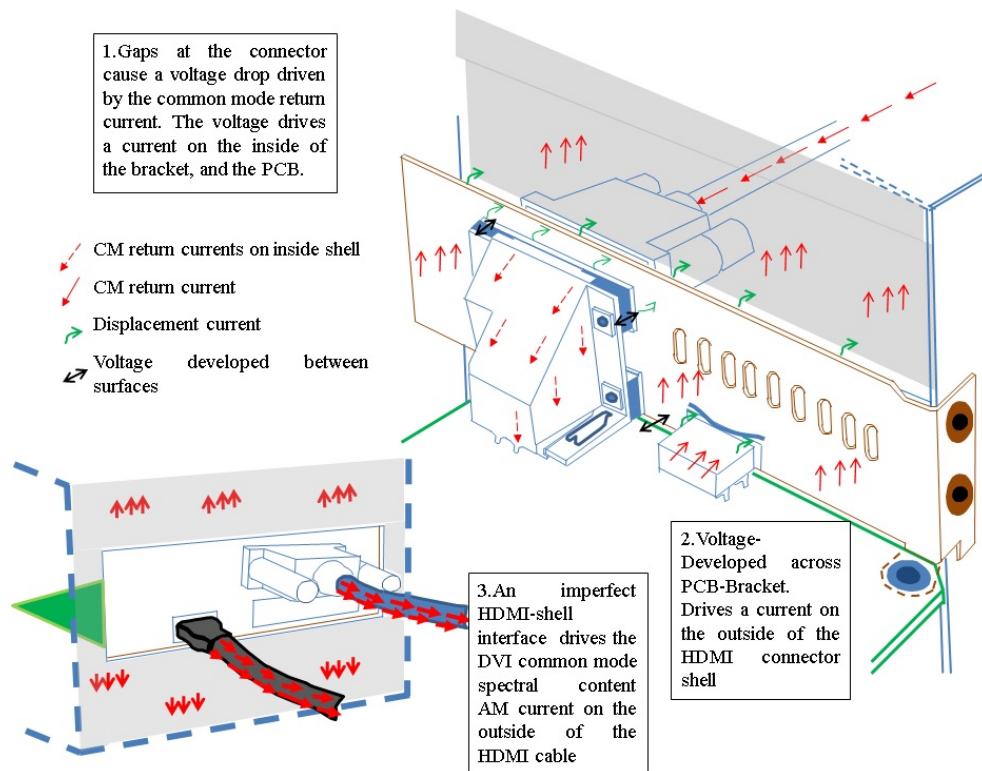
Figure 3.5. Coupling to the HDMI connector

4. QUANTIFYING THE COUPLING PATHS

A critical EMI factor is investigated such as identifying the different sources of AM currents on the DVI link in order to quantify the various coupling paths using the segmentation method employing measurement and simulation methods. This section helps in identifying which interface contributes most towards the field strength 3m away and suggest changes so as to reduce this mode conversion and coupling. The parts of the coupling path which do not have a well-defined port will need to be addressed mostly by gap voltages and simulation methods. Here one has to overcome the numerical limitations that become the limiting factor for small structures, such as the interior of the connector, the minute dimple like taps on the DVI connector, etc. for which measurement based methods are used. For quantifying the contribution from the connector-cable assembly structures a test structure is designed to measure the transfer function [Pam/Pin]. This transfer function expresses the AM current in terms of power measured on the cable shield to the input power of the system which is used along with the measured DM power spectrum to estimate the AM current on the cable attached. The same test setup is used to screen the shielding of different cables as well. However, the coupling from the connector gaps to other adjacent connectors, such as a HDMI connector will require a numerical and measurement based two-step approach. The entire study is based on such a segmentation methodology and is developed to quantify the coupling mechanisms from DVI gaps/slots to bracket slots and further to radiated-field emissions.

4.1. MODE CONVERSION WITHIN THE CONNECTOR MODULE

For the connector it is important to characterize the gap voltages so as to study its impact towards the EMI performance. In order to characterize the various

gaps on the connector, the port voltages at the various gaps on the connector body is measured using a 3 port VNA.

The measurement was performed on a test board with a dual stack DVI connector. The 3 port VNA is used to excite the test structure and measure the gap voltages at the different connector gaps. The mixed mode S-Parameters are obtained with the balanced port (DVI excitation) assigned as logical Port 1 and the single ended unbalanced port (probe used to measure gap voltages) as logical Port 2 as shown in Figure 4.1. The ports indicated in (1) refer to the logical ports defined as indicated in Figure 4.1. The naming convention for the transformation matrix (Equation 4.1) is explained in Equation 4.2.
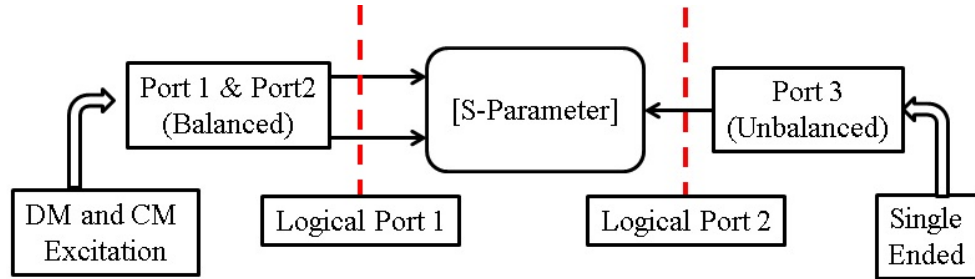
Figure 4.1. Mixed mode port definitions

$$\begin{bmatrix} S_{dd11} & S_{dc11} & S_{ds12} \\ S_{cd11} & S_{cc11} & S_{cs12} \\ S_{sd21} & S_{sc21} & S_{22} \end{bmatrix} \tag{4.1}$$

$$\begin{bmatrix} S_{ModeResponse;ModeStimulus;ResponsePort;StimulusPort} \end{bmatrix} \tag{4.2}$$

S_{sd21} is the transmission parameter that describes the amount of common mode voltage produced at logical Port 2 when there is a differential mode stimulus

at logical Port 1, which also relates to the generation of EMI. Similarly S_{sc21} refers to the gap voltage produced at a slot given a certain CM input voltage in the system.

The mode conversion is calculated using Equation 4.3 and Equation 4.4. It should be noted the ports indicated in Equation 4.3-4.4, e.g. in S_{xy}, x and y corresponds to the physical ports and not to the logical ports. Using a simple coax probe across the interface would measure the voltage at that interface for a CM excitation (S_{SC21}) or DM excitation (S_{SD21}). Figure 4.2 shows the test setup.

$$S_{sd21} = \frac{1}{\sqrt{2}}(S_{31} - S_{32}) \tag{4.3}$$

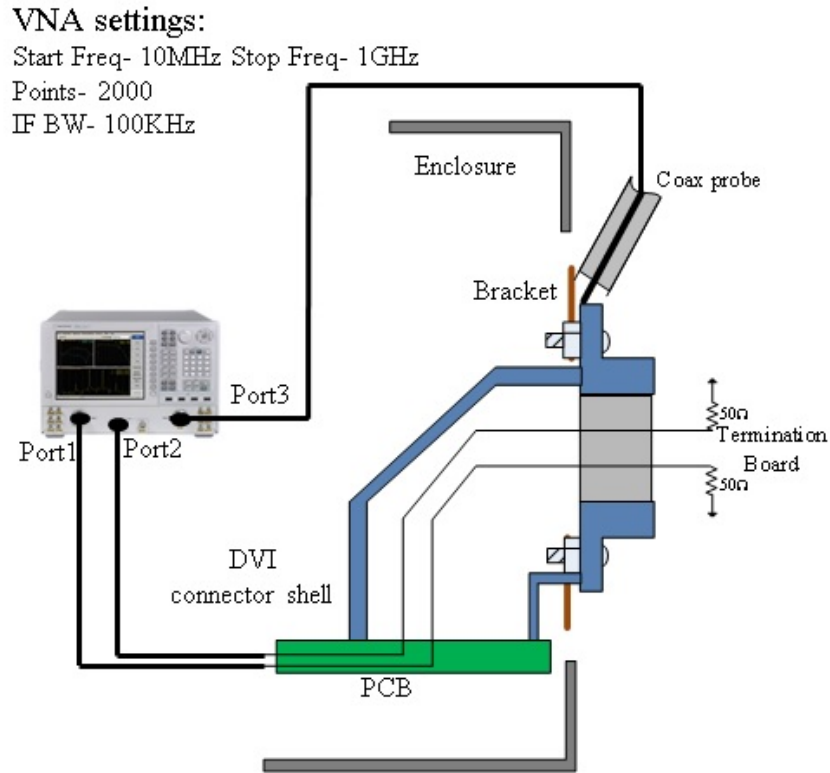$$S_{sc21} = \frac{1}{\sqrt{2}}(S_{31} + S_{32}) \tag{4.4}$$

Figure 4.2. Test setup for mode conversion on the connector body shell

The differential pair on the test board was excited using Port 1 and Port 2 of the VNA while a small coax probe was connected to Port 3 of the VNA. The differential pairs on the DVI connector were terminated using a termination board. A port extension was performed on Port 3 till the end of the coax probe. The coax probe used is shown in Figure 4.3. The coax probe was connected between the two surfaces forming a gap and the port voltage was measured.The mode conversion parameters were calculated using these measured S-Parameters. The underlying rationale for this measurement is the following: differential mode currents gets converted to common mode currents at the imperfections within the connector/cable/PCB. The common-mode return current flows through the inside of the connector body. Due to the gaps present in the shell of the connector, the common-mode return currents drive a voltage across the gaps which would drive currents on the outside of the connector shell and due to current continuity, the current flows on the inside of the bracket and enclosure of the system. Hence, this port voltage measurement can give us an estimate of the slot that contributes towards the maximum mode conversion on the body of the connector.
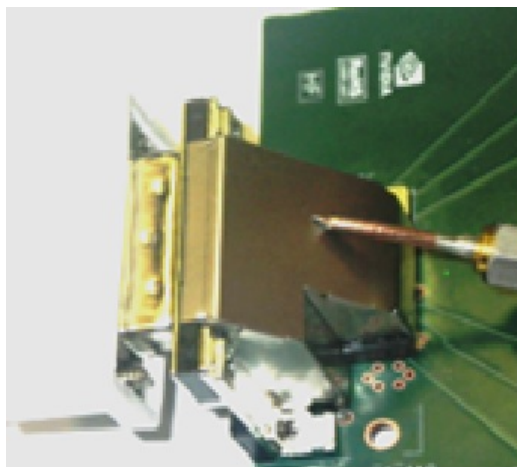

Figure 4.3. Probe used for gap voltage measurement

Some of the results are shown in Figure 4.4. As can be seen, the voltage conversion is more in the common-mode case as compared to the differential mode case.Based on the above described mode conversion results, it can be observed that the top flange-body frame contact contributes the most towards the gap voltage which in turn can drive AM currents on the outer metallic structures. In order to confirm our findings from this test, we do a relative study based on measured field strengths at 3m distance to confirm the maximum contribution of each slot on the connector body shell. The relative effect of the contributions of the different slots on the connector body is studied in the radiated emissions test setup which is the main criteria in distinguishing the effect of each slot. The effect of each slot on the radiated field is studied by making each contact imperfect one at a time when all other gaps are perfectly shielded so as to have the contribution of only one gap/slot at a time. The slots on the connector body are completely shielded using copper tape as shown in Figure 4.5.
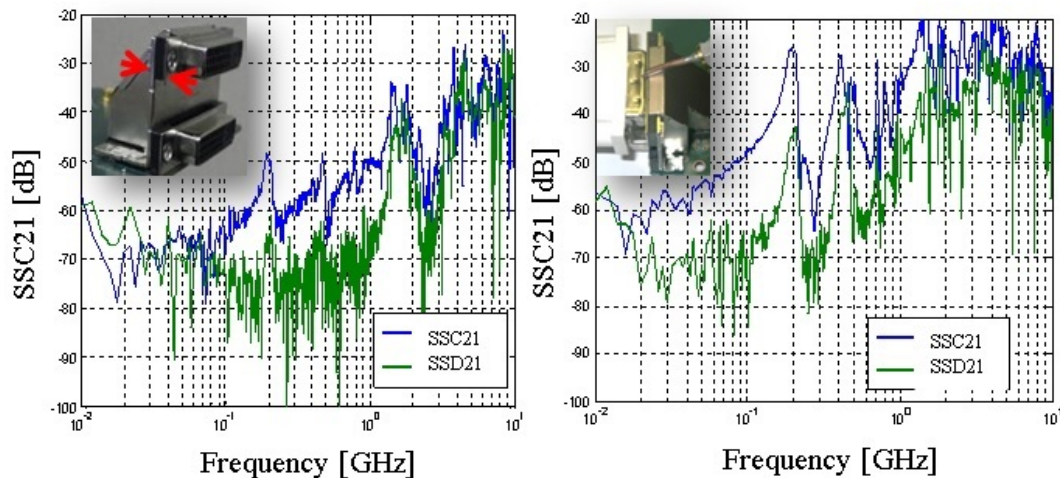

Figure 4.4. Mode conversion on the connector body shell (a) side black gaps, (b) body shell - frame contact
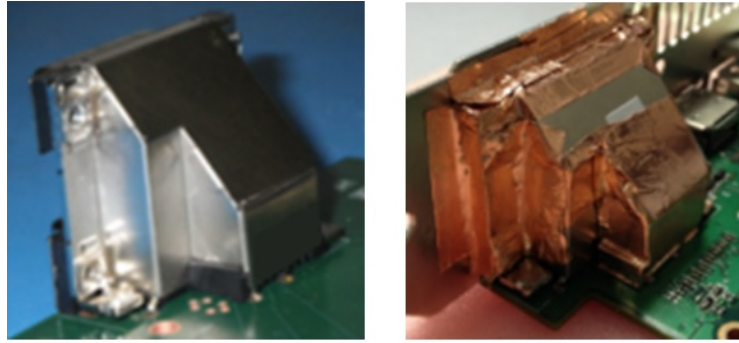
Figure 4.5. Unshielded and shielded DVI connector

This was performed on the actual system graphics card, where the system was placed inside the chamber for performing the radiated emissions test. Figure 4.6 shows the test setup. A baseline is measured with the entire connector well shielded. Each gap is then made imperfect one at a time to observe its effect in the far field emissions. A similar trend is observed on the radiated field tests where the top flange contact when made imperfect shows the maximum increase in the radiated emissions above the base case having all well shielded slots. Figure 4.7 shows the measured field strengths for all the test cases and Table 4.1. lists the field strength for each slot which can be compared to the baseline well shielded case.

Table 4.1. Field strength for different connector body shielding at 742.5 MHz

	dBμV/m
Baseline	33
Top contact unshielded	37.6
Side unshielded	33.4

Thus based on the above quick measurements based on port voltages, the most dominating slot on the connector shell body can be determined. Adapting simulation methods can also help in understanding the coupling. Simulation of the connector alone can give an insight into the performance of different DVI connectors. The
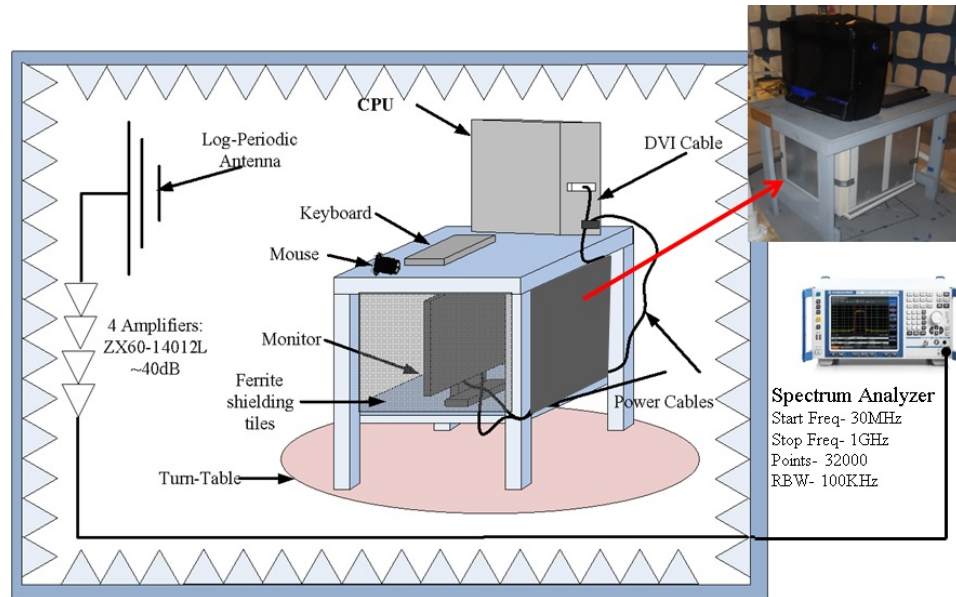
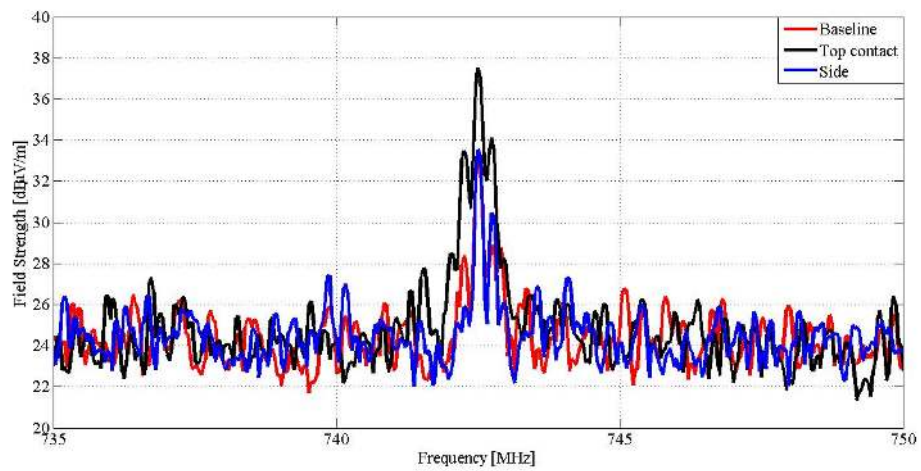Figure 4.6. Test setup for radiated field measurements

Figure 4.7. Measured field strengths for different connector body shielding at 742.5 MHz

surface current distributions can be compared when the DVI connector is excited in common/differential modes and rough judgments on which parts on the connector shell are important in the signal return path can be determined. In this simulation the connector is mounted on a simple PCB structure. The connector is terminated with matched loads at the cable end. Design changes can be suggested to improve and reduce the EMI radiations based on the surface current observations.

An additional shorting pin is attached from the connector body shell to the PCB reference plane as shown in Figure 4.8. Figure 4.9 illustrates the surface current distribution on the outside shell of two different DVI connectors. For the original connector, the surface current is strong and widely distributed on the bottom part of the metal shell of the connector. This indicates strong return currents on the connector cover, which may further induce strong radiations by exciting AM currents on the inside of the bracket-enclosure system.
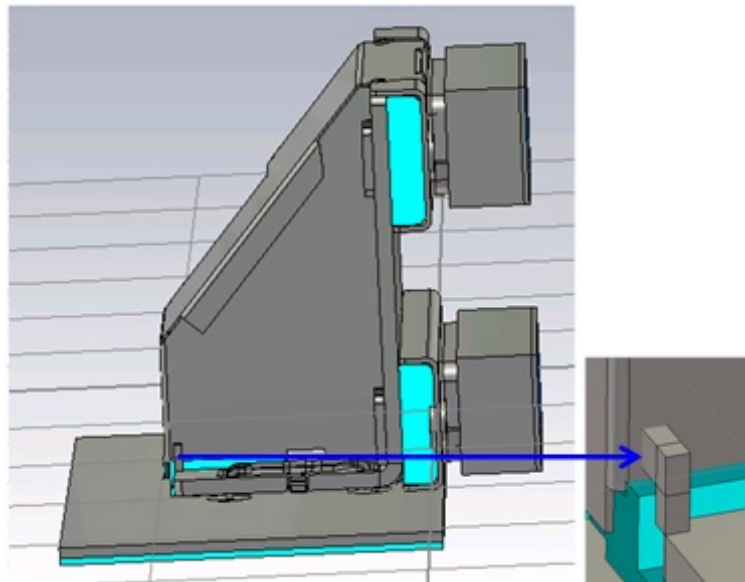

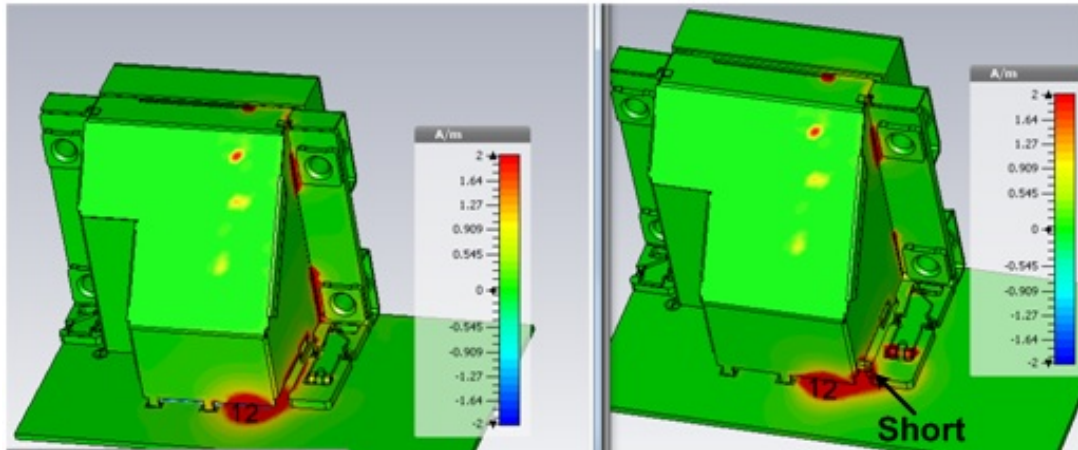Figure 4.8. Connector shield with additional GND pin

Figure 4.9. Surface current distribution on the connector shell

The additional shorting pin provides a lower impedance return path for the signals. It can be observed from Figure 4.9 that the surface current on the shell is reduced and its distribution area shrinks. Based on the above measurements and simulations, certain suggestions on the design of the DVI connector shell can be made to improve the EMI performance of the connector. The two most important suggestions are: (a) add more taps/dimples on the shield - connector frame contact. (b) add additional GND connect on the connector body shell close to the signal pins.

4.2. MODE CONVERSION IN THE CONNECTOR CABLE ASSEM-BLY

After determining the important slots/gaps on the connector body shell, next in the coupling path analysis is the connector-cable assembly structure, including the DVI connector, cable connector, the cable, all mechanical supporting structures like the bracket that holds the connector in place and the bracket-enclosure contact. It should be noted that, besides the AM currents caused by the connector body shell gaps which can leak out from the imperfect bracket-enclosure contacts, shield leakage of DVI cables could also results in strong EMI radiations. In order to capture the

effect of the imperfect interfaces which convert the CM return currents to AM currents we first need to remove the effect of the cables inherent ability towards this mode conversion.

4.2.1. Cable Shielding. Braided cable shields show a strong mode conversion through their own shield [9],[5],[16]. A simple test setup was designed to measure the shield leakage of commercially available DVI cables. The setup was then further extended to measure a transfer function between the AM current on the outside of the DVI cable to the power injected to a DVI connector in-order quantify the various interfaces. A schematic of the measurement setup is shown in Figure 4.10 to measure the shield leakage of different cables. Port 1 and Port 2 of the VNA are connected to one of the differential pairs of the connector that is located in the well-shielded small shielding box while port 3 of the VNA is used to measure the antenna-mode current by means of a current clamp or current probe through an amplifier.
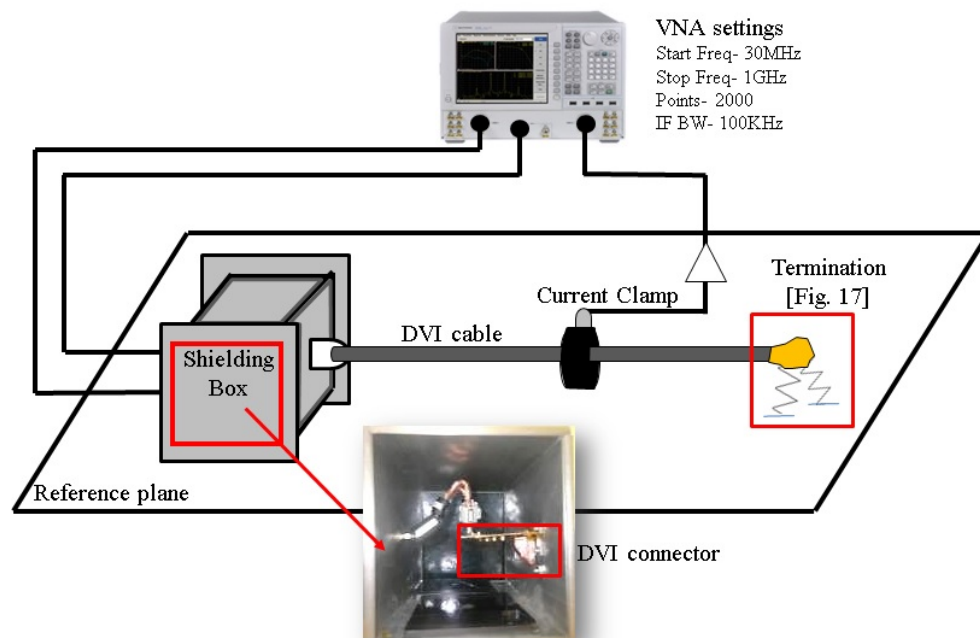

Figure 4.10. Test setup- cable shield leakage

The signal lines of the DVI cable are terminated with a matched load of 50Ω to the shield of the DVI cable as shown in the Figure 4.11. In the same figure we see the signal reference is terminated to the shield of the DVI cable. The shield of the DVI cable is at a certain height above reference plane forming a transmission line structure whose characteristic impedance is 235Ω. To avoid reflection of antenna-mode current along the shield of the cable, two 470Ω resistances are connected in parallel to match the transmission line. The current on the shield of the cable is measured by moving the current clamp along its length. The currents driven by connector gaps are distinguished from the currents caused by shield leakage by observing the current distribution along the cable into the termination. A current that is driven by a connector gap will have a constant magnitude from the connector to the termination, as there is no reflected wave. However, distributed leakage will excite currents along the length of the DVI cable, thus, leading to a strongly fluctuating current magnitudes along the DVI cable.
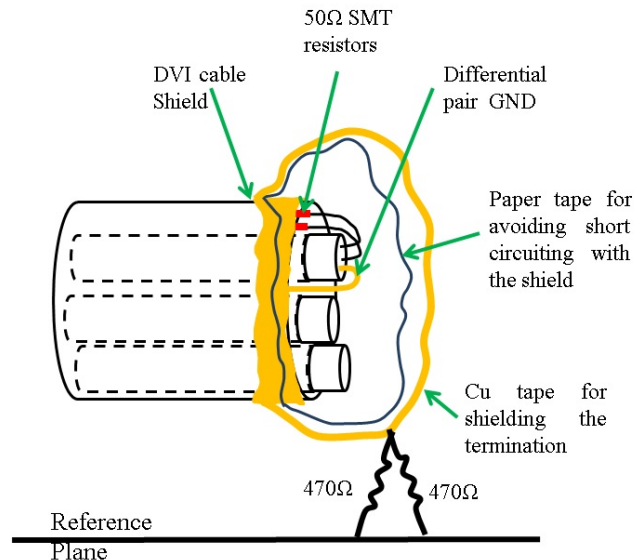
Figure 4.11. DVI cable termination

The mode conversion (S_{sc21}) is calculated by using the single ended S-Parameters measured using the VNA. By varying the current clamp location along the length of the cable, the mode conversions of two different cables are compared in Figure 4.12,4.13. A constant and low mode conversion along the length of the cable shows better shielding effect for that DVI cable. This experimental setup can be used to select better EMI shielding DVI cables by analyzing the mode-conversion. Clearly the Dual link DVI cable shows better performance compared to the standard off the shelf DVI cable (Figure 4.13). Dual link DVI signals have a higher operating clock frequency range [1]. This may be the reason for the cable marked dual link to be designed for better shielding capabilities.

In order to distinguish the AM currents along a cable due to the imperfect metallic connections from those caused by leakage of the cable, a well-shielded cable is made by modifying DVI cable 1. The plastic cover around the cable shell and the outer protective sheath of the entire cable was removed. A 360° connection of the shield to the DVI cable connector shell was made using copper tape that was then extended to the entire length of the cable making a solid cable shield as compared to the previous braided cable shield. The same test is repeated using the cable with the modified solid shield. This lowered the shield leakage significantly for the cable under test.

Figure 4.14 shows the mode conversion (S_{sc21}) for the same cable as shown in Figure 4.12 after the modified solid shield. It is observed that for the well-shielded cable, the mode conversion (S_{sc21}) is extremely low and constant along the length of the cable with the variation of the location of the current clamp. With the contribution removed from the poor shielding cable, we can now use the same test setup to measure the currents driven on the cable shield by the imperfect contacts at the connector-cable assembly structures.
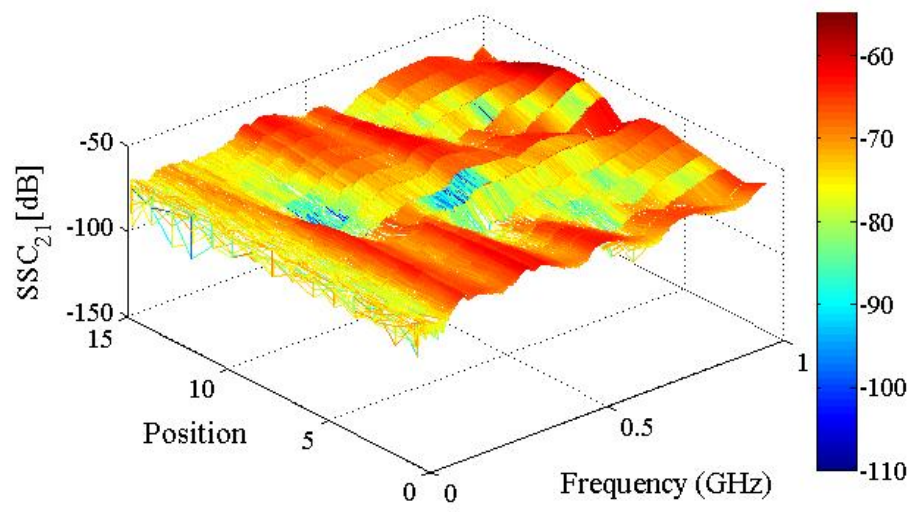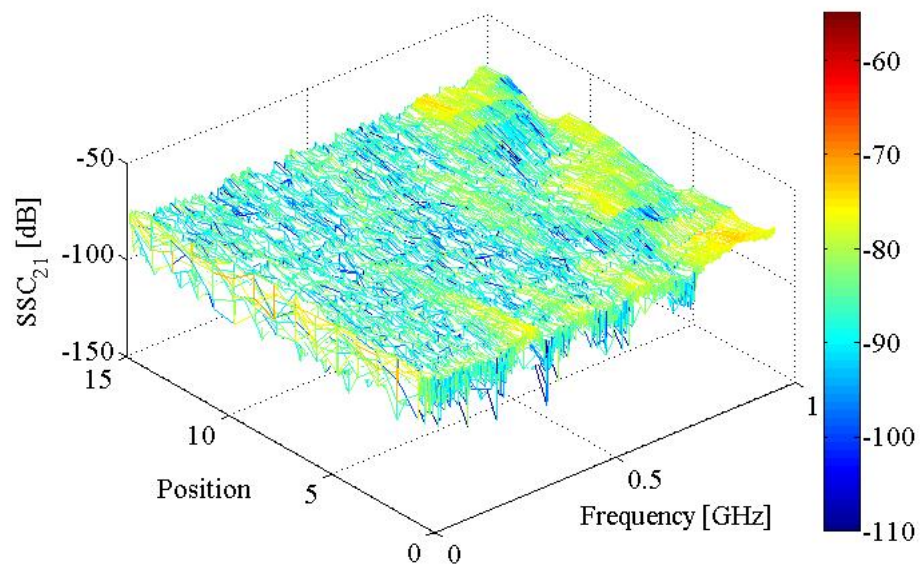
Figure 4.12. Shield leakage cable 1

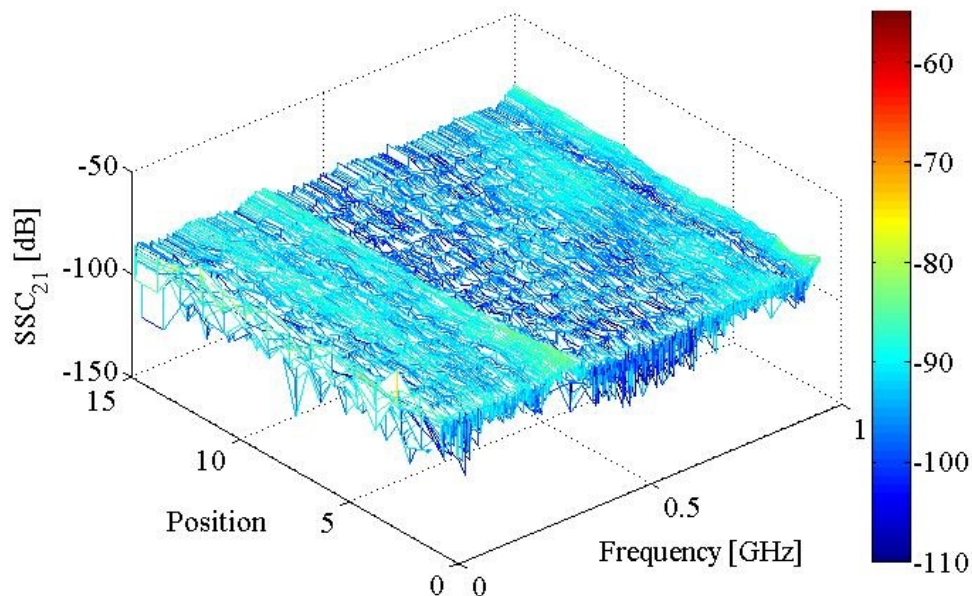

Figure 4.13. Shield leakage cable 2

Figure 4.14. Shield leakage after proper shielding - cable 1

4.2.2. Connector Cable System. The imperfect contacts (at the interfaces: Figure 2.2 (A) DVI connector shell- DVI cable shell, (B) DVI connector shell-Bracket, (C) Bracket-Enclosure) can convert the CM return currents to AM currents flowing on the outside of the DVI cable or the metallic computer enclosure, which are efficient radiating structures. The connector shell and the cable shell are connected through six contact points (dimples) - three on the top and three on the bottom, hence it is not a perfect 360° connection and has just a few contact points on the top and bottom of the shell-shell interface. The DVI connector-bracket is held together by four screws, two screws on each DVI connector level. Hence this connection is not perfect as well. Moreover, the bracket-enclosure contact is using two screws and gasket enforced connections along the length.

The same setup with the well shielded DVI cable can now be used to determine a transfer function which defines the ratio between the AM current on the outside

of the shielded DVI cable to the differential input power into the system (Iam/Pin). Instead of using a VNA to measure the S-Parameters, we now use the tracking generator as a source to generate the broadband input power, which is fed into a hybrid. The differential outputs of the hybrid are connected to one of the differential pair inputs of the connector test PCB (Figure 4.15). The idea behind this setup is to excite the connector system in DM and obtain the AM on the cable shield due to each imperfect contact in the system. The power received using the current clamp is then converted to current using the transfer impedance of the probe. This test was performed for the DVI connector shell-cable shell, shell-bracket and bracket-enclosure interfaces.

Each case was performed one at a time, for example when the shell-shell contact was made bad, all other contacts, i.e. the shell-bracket, bracketenclosure contacts were perfectly shielded using copper tape. This ensured the contribution from one imperfection at a time. A transfer function of each connector joint is derived using the injected power and measured current on the DVI cable. Figure 4.16 shows this TF.
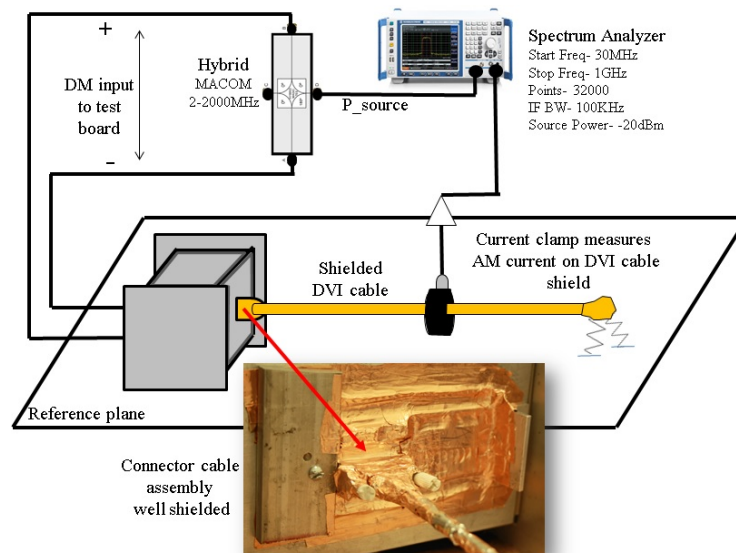

Figure 4.15. Test setup to measure the mode conversion for the different interfaces

Based on the measurements it is observed the shell-shell contact to be the most important contact in the connector-cable assembly as for the same power injected, maximum AM current is measured on the cable. For estimating the impact of these imperfect interfaces, the radiated fields need to be estimated. The TF enables us to estimate the AM current on the cable given a certain input DM power spectrum. The measured DVI DM spectrum is used as an input and the AM current on the cable is estimated for each case and the radiated emissions estimated and compared to the actual system emissions. The input power that is used as an input to the transfer function is the DM power spectrum measured on the graphics card before the connector. Figure 4.17 shows the measurement on the graphics card where the probes are connected before the connector by removing the decoupling capacitors. The probes connect to a hybrid which gives us the DM spectrum measured at the SA input. Using this measured power spectrum, the AM current is calculated for the three cases. This antenna-mode current is then used as the current source in order to obtain the radiated field from using a simple dipole assumption [6].
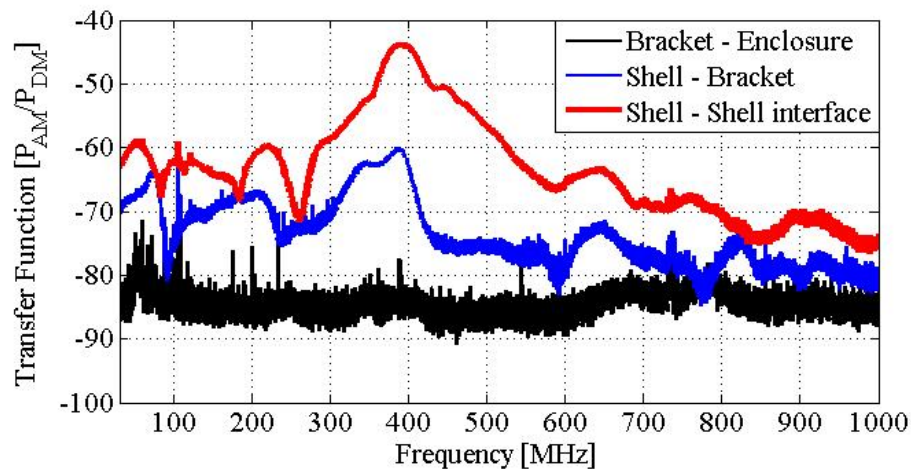

Figure 4.16. Transfer function for different interfaces
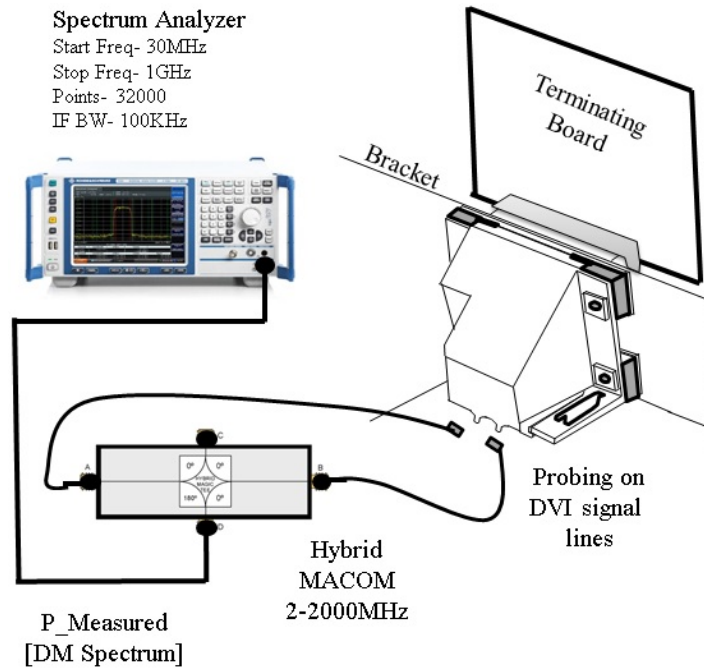
Figure 4.17. Test setup to measure the input DM power

For validating our estimation of the radiated field emissions, similar modifications were made on the connector-cable assembly on the real system and the maximized radiated fields were measured in the anechoic chamber. For example, for the shell-shell interface, it was made imperfect using mylar tape while all other gaps were properly shielded using copper tape. Figure 4.18 shows the estimation for the DVI clock frequencies at 742.5 MHz compared to the actual measured case. The estimation is in the range within 5dB compared to the actual measured values. Equation 4.5 assumes constant current flowing along the entire length of the cable and estimates the radiated field at a distance of 3m from the wire.

$$E = \frac{4\pi 10^{-7} f i L Sin\theta}{r} \tag{4.5}$$

f- Frequency I-Antenna-mode current L-Length of cable - Azimuthal angle r-Observation distance.

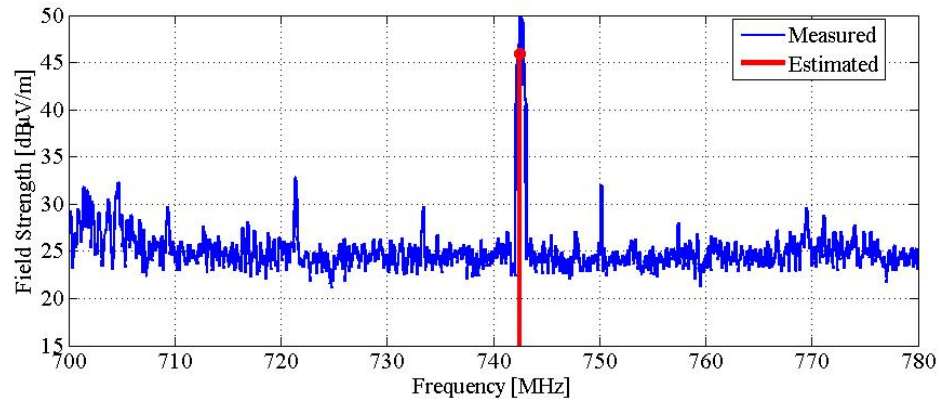Using similar methods, the field strengths at other important frequencies can be estimated as well.

Figure 4.18. Comparison of the estimated and measured field strengths at 745.5MHz

4.3. COUPLING TO ADJACENT CONNECTORS

A high speed connector can have other connectors adjacent to it on the same PCB and mounted on the same bracket. The coupling to adjacent connector has been studied here taking an example of an HDMI connector mounted on the same PCB sharing the enclosure mounting bracket with the DVI connector. An assumption is that there is no coupling from the outside of the enclosure, ex. from the DVI cable to the HDMI cable. This section focuses on how the coupling from a DVI connector to a HDMI connector-cable system results in antenna mode (AM) current on the HDMI cable having the DVI common mode (CM) spectral content. The coupling to the adjacent HDMI connector is mainly caused due to the CM return currents of the DVI link system via two coupling mechanisms. Coupling may occur inside the PCB, e.g. the DVI signals can excite a power ground plane cavity which propagates the signal

to the HDMI signal at a HDMI via transition through power ground plane. This would lead to the DVIs spectral content becoming visible on the HDMI signal, but not necessarily to an antenna mode on the HDMI cable having DVIs spectral content. The second coupling path is outside the PCB, but inside the enclosure and is caused by the imperfect shielding of the DVI connector and imperfect contact of the HDMI connector shell taps to the bracket (Figure 4.19). This is studied by considering a scenario where there is no direct EMI issue caused by the DVI connector-cable system. The study is scenario based where the DVI connector is active and connected to a display monitor through a very well shielded high quality cable. In this DVI link the CM currents may arise due to the transceiver, imperfect symmetry of the differential signal paths, asymmetric termination at the load end, etc. The contacts at the DVI connector on the PCB to the DVI cable are very good and the connector-cable shield connects to the chassis ideally. This scenario is considered, as this would eliminate the direct contributions of the DVI connector-cable system towards EMI problems.
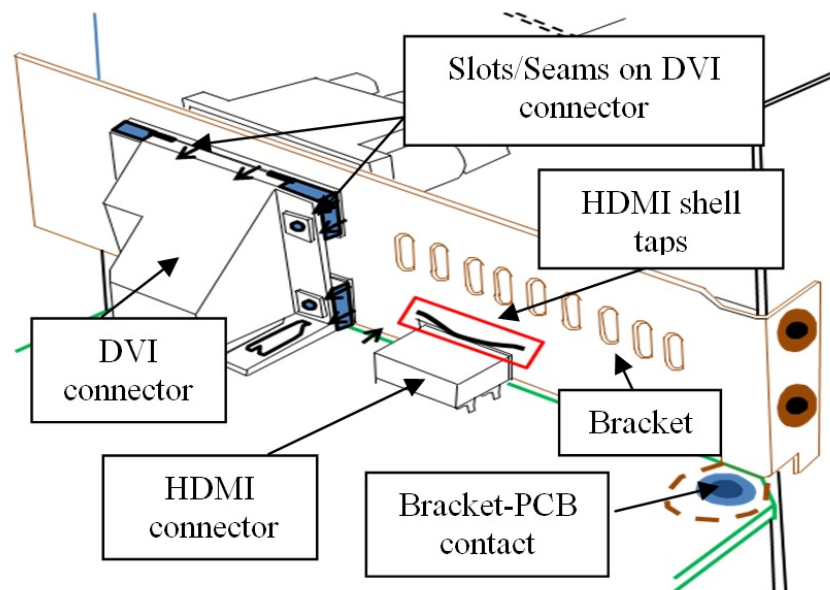

Figure 4.19. DVI and HDMI connector-bracket system

On the other hand, on the inside of the enclosure, the DVI connector shell is not perfectly shielded and has some seams and slots for mechanical mounting reasons. These gaps on the DVI connector shell will cause a voltage drop driven by the CM return currents [12],[14]. This voltage would drive a current on the inside of the bracket and the PCB. Due to the imperfect contact at the HDMI shell-bracket interface, a voltage will be developed at this interface which would drive AM current on the outside of the HDMI cable attached, with a DVI CM spectral content.

4.3.1. Internal Coupling vs External Coupling. To compare the different coupling paths, two separate simulation models are setup where the internal coupling model (Figure 4.20) includes part of the real PCB, the bracket and the HDMI connector and the external coupling model (Figure 4.21) includes a solid plate representing the PCB, the bracket and the HDMI connector with contact taps to the bracket. In both the models a 200Ω resistor is used as a HDMI load between the 'HDMI cable shield' and the HDMI shield box (Figure 4.20-B) to quantify the coupling noise by observing the coupled current in the HDMI load resistor. In the internal coupling model, the DVI connector is removed and all signal lines are match terminated. On the HDMI side, the HDMI signal lines are similarly terminated.
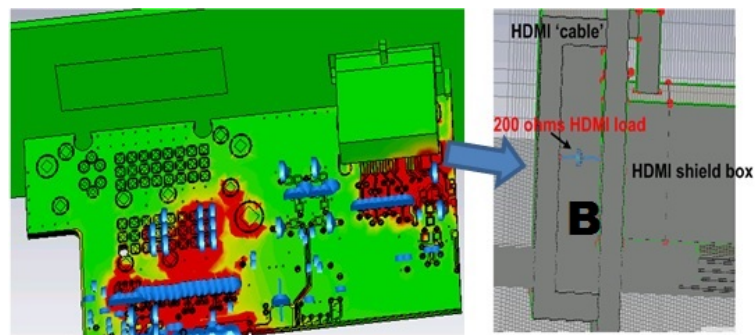

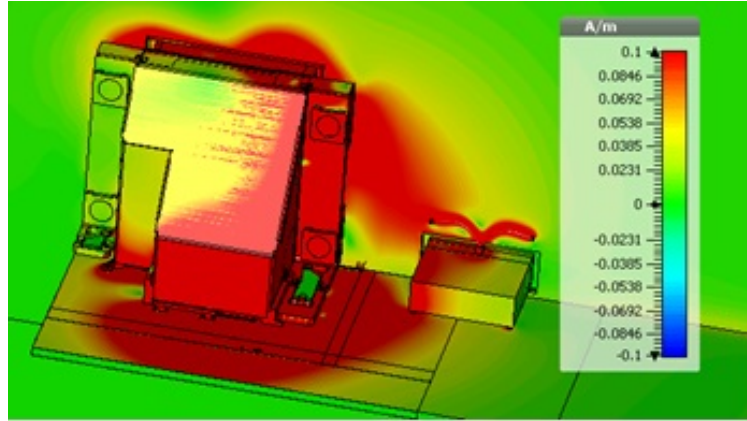Figure 4.20. Surface current distribution for internal coupling

Figure 4.21. Surface current distribution for external coupling

The idea is to observe how much signal from the DVI gets coupled to the outside of the HDMI cable shield due to the internal board geometry. Though there may be some coupling to the actual HDMI signal lines, the AM current due to this internal coupling is rather weak. This statement is validated in the following simulation setup. One differential pair in the DVI link is exited in CM to obtain the coupling in the HDMI connector side. From the surface current distributions it can be seen that the DVI common-mode signal may cause noise current distribution on the HDMI connector pin field. The coupled current on the 200Ω resistor is the parameter used to evaluate the coupling strength. The external model contains a solid plate to represent the PCB, the DVI connector, the bracket and the HDMI connector (Figure 4.21). With the same CM excitation, current distributions and current through the HDMI load resistor is observed.

The coupling currents in the 200Ω resistor for two models are compared in Figure 4.22. It can be seen that the external coupling is much stronger than the internal coupling through the PCB. This indicates the noise suppression for the external coupling paths are more important than those of the internal coupling. Once
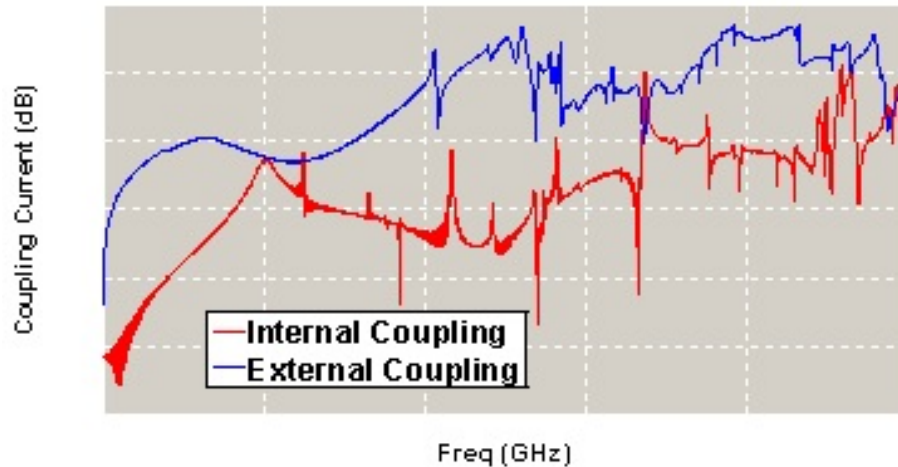
Figure 4.22. Coupling current in 200 Ohm resistor

it is certain that the external coupling path dominates, an effort has been made to quantify this external coupling path.

A measurement based method to quantify the mode conversion from differential signaling of the DVI connector to AM current with a DVI common mode spectral content on the HDMI cable is investigated. This is achieved by measuring the S-Parameters and then formulating a power transfer function model based on the coupling, which predicts the coupled power to an equivalent load resistance (R_L) between the bracket and the HDMI connector shell assuming a perfect contact at the HDMI cable shell-connector shell interface. This coupled power is used to derive the AM current on the cable attached to the HDMI connector which would radiate based on a radiation resistance (R_{rad}) that is used to derive the closed form estimate of the radiated field emissions.

4.3.2. Coupling Path Characterization. The coupling between the DVI connector and the HDMI connector can be defined in terms of S-Parameters. The S-Parameters can be used to extract the coupling information based on the way the ports are defined in the system. A port can be defined where it is possible to have a

well defined voltage and current [17],[18]. Thus the selected two-terminal port needs to be either electrically small in dimension as compared to the wavelength of the highest frequency of interest, or support a TEM wave. Considering a two port system if one port is defined at the noise source excitation end (DVI) and the other at the coupled victim's end (HDMI), the S-Parameters will contain the coupling information needed to be able to quantify this coupling. In this case the HDMI cable being the major antenna structure, the voltage between the connector shell and the bracket connected to the enclosure is mainly important. Hence the victim side port is defined between the outer ground shell of the HDMI connector shell and the nearest point on the bracket where it is possible to measure this port voltage. The DVI connector source can be defined as the excitation port.

The differential signaling by itself will cause weak emissions, the CM currents that further get converted to AM currents cause significant EMI issues as discussed earlier in Section 2. The mixed mode S-Parameters will help us in characterizing this mode conversion. The mixed mode S-Parameters (Equation 4.1) are obtained when the balanced port (DVI excitation) is assigned as logical Port 1 and the single ended unbalanced port (between HDMI connector shell-bracket) is logical Port 2 as shown in Figure 4.1 earlier. Once the Mode conversion has been measured the idea is to obtain a power transfer function that would define the coupling between two adjacent connectors. Once the single ended S-Parameters are measured and the conversion term derived, Equation 4.6 is used to determine the ratio of the power dissipated in the load resistor (R_L) to the source power input to the system [18]. A good approximation for the equivalent contact resistance can be used to estimate the current which is the AM current on the shield of the HDMI cable when the cable is assumed to be connected to the HDMI connector.

The power transfer function, 'G' is defined as the ratio of power dissipated in the load (Z_L) to the power delivered to the input of the two port network (Figure 4.23).

In Equation 4.6, S_{21} is the measured coupling S-Parameter function (S_{SD21} when exciting the DVI connector in DM or S_{SC21} when in CM), Γ_{in} and Γ_L are the reflection coefficients at the input and load terminals respectively. The above transfer function along with the mixed mode S-Parameters is used to determine the power dissipated in the load resistor (P_L). As a check we know if the network is totally matched then all of the magnitudes of the reflection coefficients are zero and the power gain, was verified with our formulation and data handling. The power equation using single ended S-Parameters has also been verified with measurement data illustrated later.
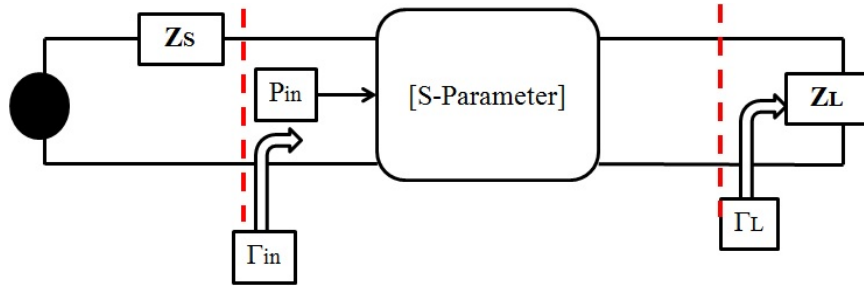

Figure 4.23. Power delivered to load

$$G = \frac{P_L}{P_{in}} = \frac{|S_{21}|^2(1 - |T_L|^2)}{(1 - |T_{in}|^2)|1 - S_{22}T_L|^2} \tag{4.6}$$

4.3.3. Simplified Test Structure. Two simple test structures are designed and the closed-form estimation has been compared to the measured radiated field emissions. The first test structure has a first level approximation for the DVI as well as HDMI connector. This model has been validated with a simulation model in order to understand the coupling mechanism better since the simulation gives more

flexibility in making changes. Once this model has been validated, a more complex test structure with real connectors mounted on a PCB has been used.

For designing the test structures in order to analyze the coupling between the connectors, multiple aspects of the structure need to be taken into account especially the structure of the excitation connector, the victim connector, the PCB and the common bracket that holds the connectors to the enclosure. The first test structure is designed considering the most simplified case of a DVI connector. Only two pins of a DVI connector, Tx1+ and Tx1- are modeled as transmission lines using coaxial cables and another GND pin is added alongside for providing a return current path. The bracket is modeled as a solid copper plate on which the simplified DVI pins are directly terminated using 50Ω SMT resistors. The shape of the co-ax cables is modified in order to have the same arrangement as for the top connector of a dual stacked DVI connector. The spacing between the co-ax cables is maintained as in proportion to the real DVI connector pins. The return path for these currents would not only be through the adjacent ground pin but also through the bracket contact with the PCB. It should be noted that all these assumptions are made not only to capture the coupling between the connectors but at the same time keep the test structure rather simple to mechanically construct as well as simulate before moving onto the more complex real connectors. For modeling the HDMI connector shell, the first level approximation is a small brass piece protruding out of the HDMI slot on the bracket. With the test structure now built, ports needed to be defined. Two ports are defined at the two driving ports of the DVI connector, while the third port is defined between the HDMI connector shell and the bracket (Figure 4.24). The Port 3 will measure the voltage developed at that location when Port 1 and Port 2 are either driven in single ended mode, common mode, or differential mode.
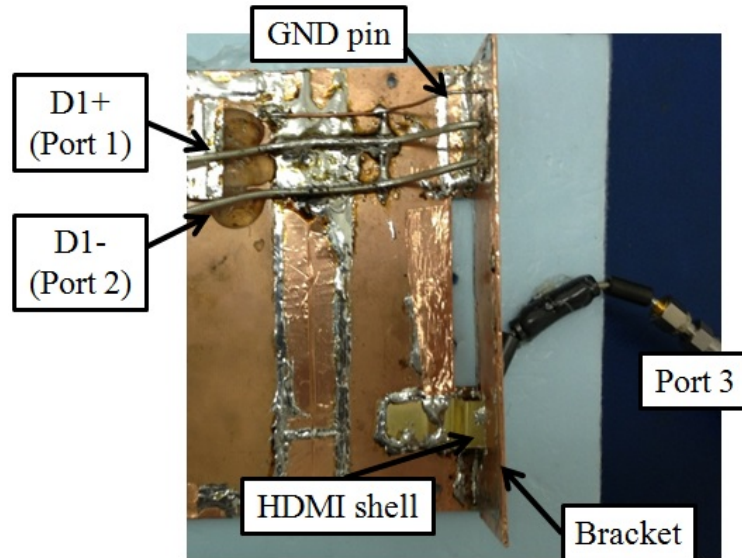
Figure 4.24. Simplified test structure for DVI and HDMI connectors

Simulation model: The simulation model is set up similar to the measurement test structure. Once the network parameters between the simulation model and the test structure can be validated, the effect of certain modifications in the simulation model can provide a better insight into the coupling and how to reduce this coupling. Such modifications included but are not restricted to a vertical slot on the GND plane, improved contact of the HDMI connector shell to the bracket using taps of different designs, shield on a DVI connector, placement of magnetic material to guide any magnetic field lines towards the victim connector, etc. Figure 4.25 is similar to Figure 4.24 where two coaxial cables define the DVI connector pins terminated on the bracket directly using lumped elements. The unbalanced, Port 3 is similarly defined between the connector shell and the brackets.

Model validation: Once the Z-Parameters and S-Parameters for the measurement and simulation model are validated, the test for understanding the coupling and making modifications to the HDMI connector shell contacts to the bracket is studied in detail using the simulation model and observing the current distributions. Figure
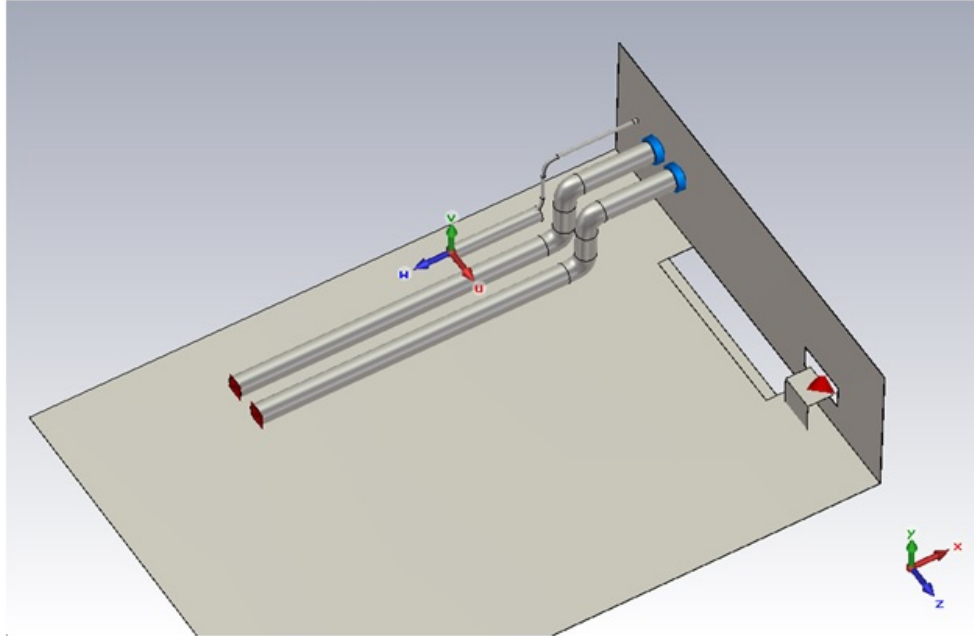
Figure 4.25. Simulation model

4.26 through Figure 4.28 shows the impedance parameters validation (derived from the S-Parameters) of only Port 1 of the DVI connector along with the validation of the unbalanced Port 3 on the victim side. Port 2 of the DVI connector was similarly validated with measurements. Figure 4.29 shows a good correlation between the measured and simulated single ended coupling S-Parameters.

As seen from the coupling Z-term, Z_{31} in Figure 4.28, at low frequency the coupling is mostly inductive with a 20dB/dec increment. This can be attributed to the time varying currents on the DVI connector-bracket loop generating a time varying magnetic flux which couples to the CM return current loop at the HDMI connector shell - bracket loop [4],[19]. An equivalent spice model with mutually coupled inductors has also been studied and validated with measurements for simulating this coupling between the simplified connectors.

One major test included having good contacts to the bracket from the HDMI shell which showed significant reduction in coupling. In the real product there exists
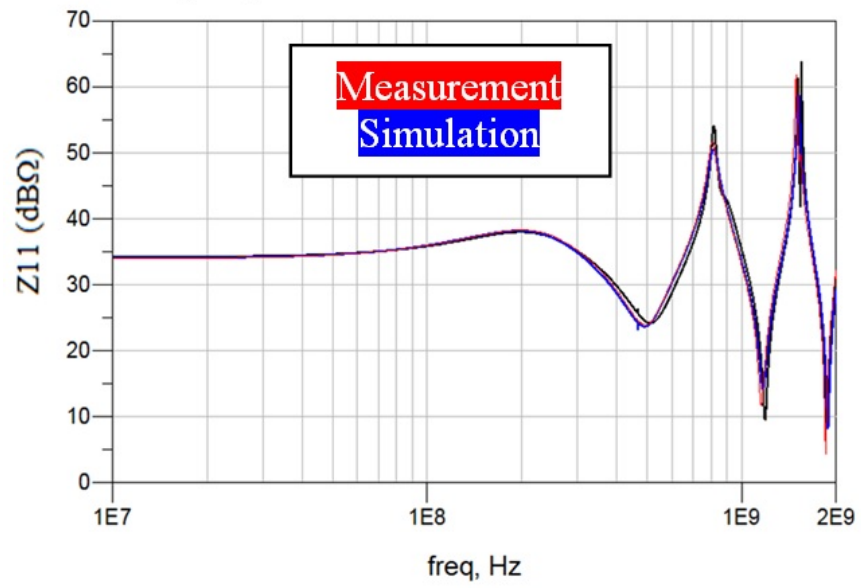
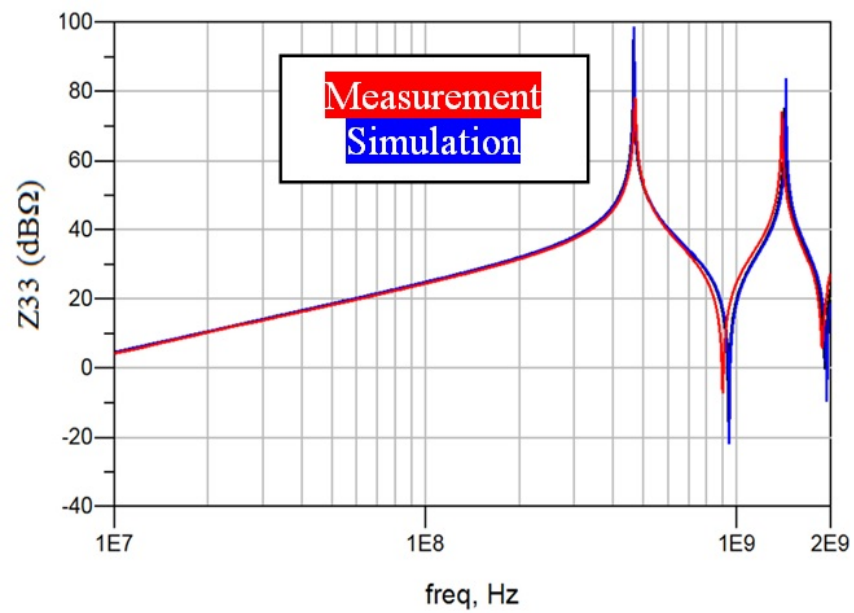Figure 4.26. Self Z-term of DVI port

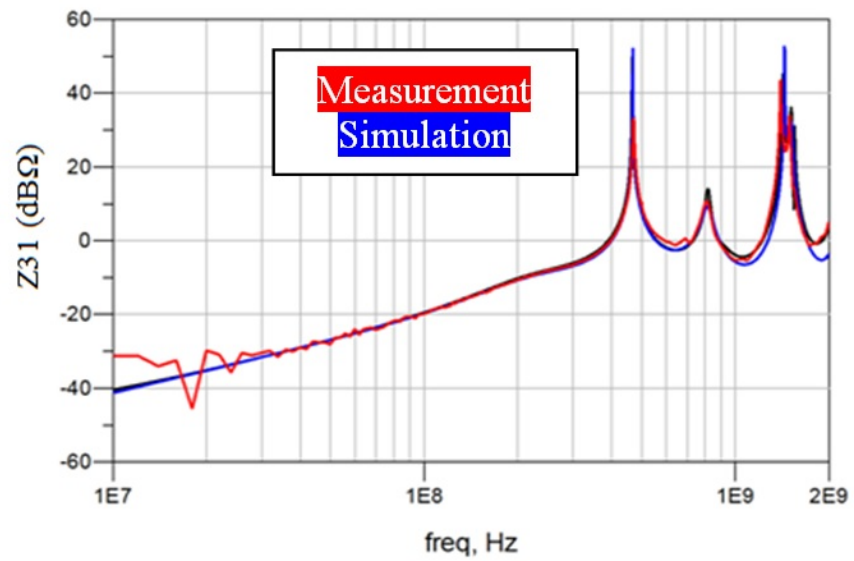Figure 4.27. Self Z-term of HDMI port

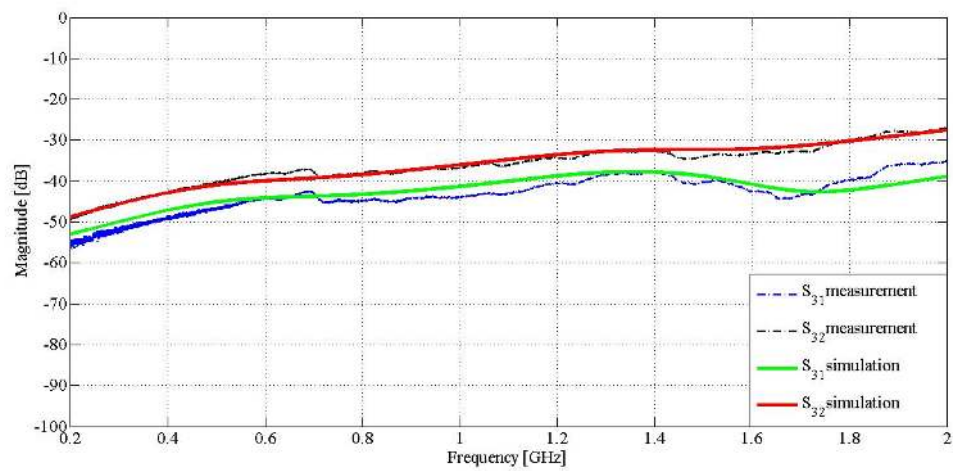Figure 4.28. Coupling Z-term validation - DVI to HDMI port

Figure 4.29. S-Parameter validation - DVI to HDMI coupling

spring loaded taps, which at times make contact but most of the time due to some mechanical mounting issues, do not make any good contact [14]. From a return current perspective, this imperfect contact at the HDMI shell to the bracket can be considered as an equivalent inductance as the current now is constricted compared to a very good contact between the connector shell and the bracket. The potential drop developed across this imperfect contact would be the source of the AM current being driven on the cable shield when a cable is attached to the HDMI connector. A method to make this contact more effective would be to have more spring loaded contacts along the sides of the shell in addition to the one present or have a 360° contact around this connector using EMI gaskets. With the HDMI connector being modeled as a short brass piece protruding out from the slot, for emulating a HDMI cable shield, 1" thick copper tape was attached to the HDMI connector, or brass piece as in this simplified model for measuring the radiated field emissions.

Radiated field tests: Before performing the radiated field test of the test structure, it is necessary to verify the power delivered to a known load in the power transfer function (Equation 4.6). In order to verify this, a signal with a certain power level is injected using the tracking generator of the spectrum analyzer at port 1 on the test structure and the power received at the HDMI port, port 3 is measured. The same power is used in the analytical model taking into consideration a load resistance R_L=50Ω of the spectrum analyzer and the power delivered to the load is calculated using Equation 4.6 and compared with the measurement data. The analytical calculation is in good agreement with the measurement (Figure 4.30). With the power equation validated, the radiated field test is performed inside a semi-anechoic chamber. For performing the radiated field tests, the test board is enclosed in an enclosure to avoid measuring direct PCB emissions. The bracket is firmly held to the enclosure using screws and finally all seams are well shielded as shown in Figure 4.31.
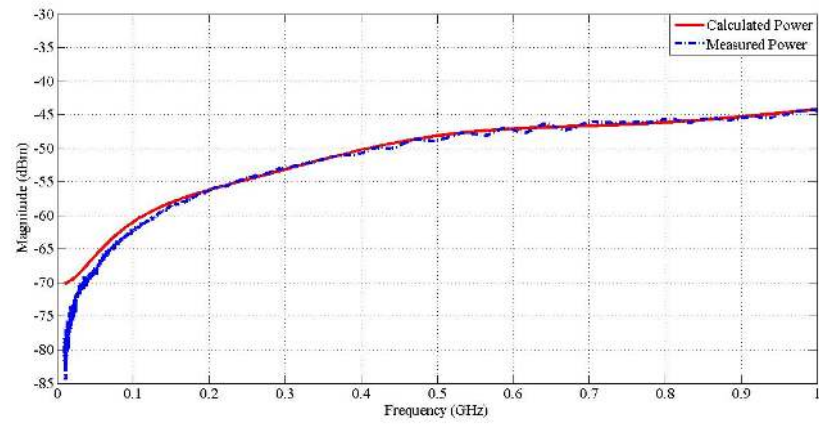
Figure 4.30. Power calculation using S-Parameters and measurement at HDMI port when DVI connector is excited with known power level
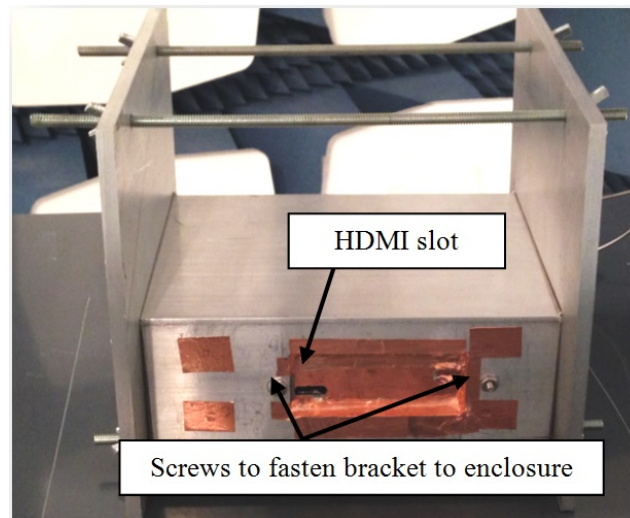

Figure 4.31. Shielding enclosure for test boards

Near field probing showed no leakage except close to the HDMI slot interface which was intentionally left open for attaching the dummy HDMI cable. For exciting the DVI connector prototype, a tracking generator of a spectrum analyzer is used with an input power, P_{in} = -3dBm. This value is to be used with the analytical model for estimation purposes. A hybrid is used when the test board is excited in CM and DM. The test board is first tested with single ended excitation, but then also in CM and DM. As the study is focusing mainly on the DVI signal using differential signaling, only the differential case has illustrated. But the same idea can be used for any single ended excitation model. The standard FCC radiated field emissions test at 3m distance is performed taking into account the antenna factor and cable loss. For the estimation process once current in the load resistor is derived, using Equation 4.7 the closed-form estimation of the radiated field emissions is derived. The closed-form estimation with the variation of the radiation resistance is indicated in Figure 4.32.

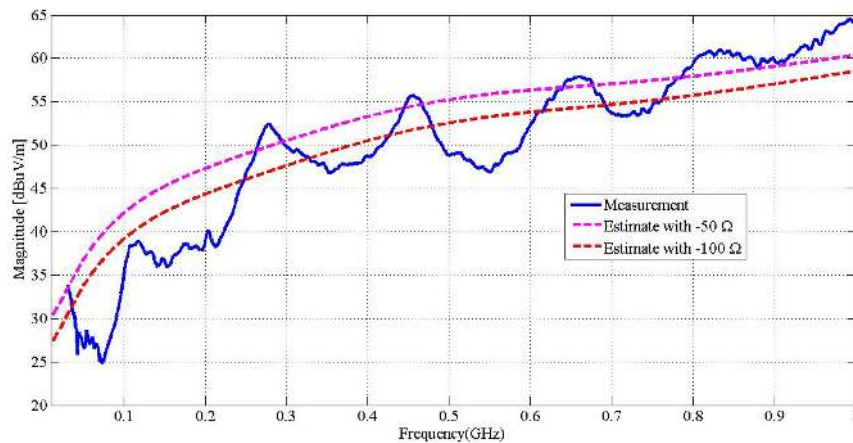$$E = \frac{\sqrt{30PG}}{R} \tag{4.7}$$

Figure 4.32. Measurement and estimation of radiated fields for simplified test structure

This method of estimation assumes all the power is radiated, which may not be true in the actual measurement case. As the S-Parameters of simulation and measurement shown in Figure 4.29 were shown to be a good match with the measurements, for estimation purposes here, the S-Parameters from the simulation model is used as it has better dynamic range at lower frequencies.

4.3.4. Test Structure With Real Connectors. With the successful validation of the estimation method using the first level prototype of the connectors, a new test board is manufactured with two high-speed connectors placed adjacent to each other as shown in Figure 4.33, one being a dual stack DVI connector and the other a standard HDMI connector. The HDMI connector has spring-loaded taps that connect to the bracket holding the two connectors [12]. The bracket has a provision to be connected to the PCB at one extreme end at the HDMI connector side, away from the DVI connector as illustrated in Figure 4.33. In this test structure the DVI signals are terminated by 50Ω resistors (Figure 4.34) and then well shielded. The entire board is then placed inside the same shielding box with the bracket being held to the enclosure with screws. Port 3 is similarly defined between the HDMI connector shell and the bracket which is attached to the enclosure as seen in Figure 4.35.
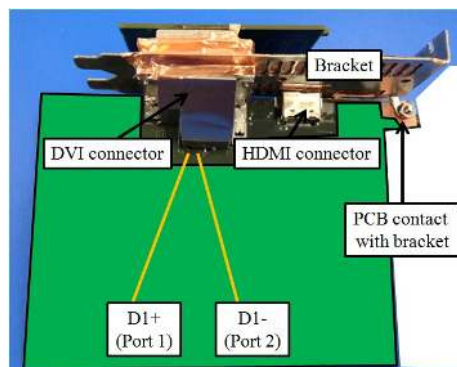

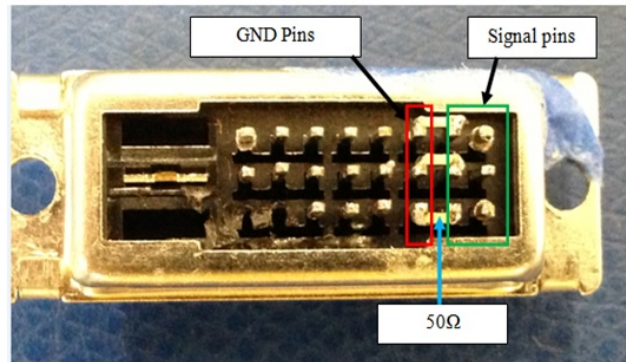Figure 4.33. Test structure with actual DVI and HDMI connectors

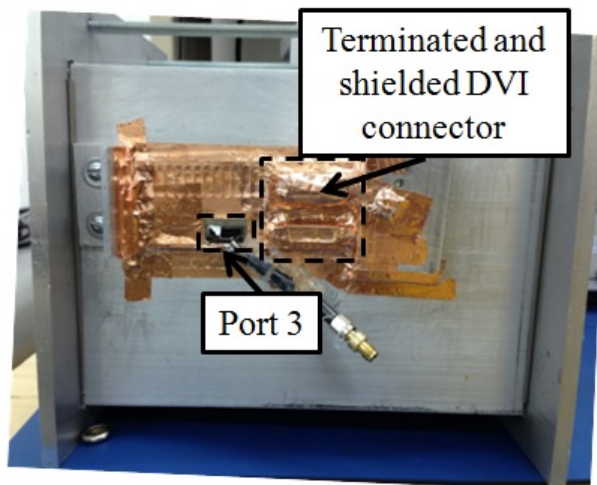Figure 4.34. Termination plug for DVI connector

Figure 4.35. Single ended port 3 location between HDMI connector shell and bracket

The same measurements are again repeated to measure the coupling from the terminated DVI signal to the HDMI connector-bracket interface. The single ended S-Parameters measured are converted to mixed mode S-Parameters which are then used in the power transfer function model (Equation 4.6) in order to estimate the current through the load, i.e. when the HDMI cable is attached to the system and with Equation 4.7 to predict the field strength 3m away. For radiated field tests, a real HDMI cable is connected to the HDMI port. Pair of signal lines of the DVI connector are then driven using a hybrid in common mode and differential mode from the tracking generator of a spectrum analyzer. For similar reasons as stated earlier, only the differential mode case has been illustrated. The radiated power received is maximized for different heights and polarizations as the DUT is rotated 360° on a turn table.

In Figure 4.36 the measured radiated fields show some cable resonances which cannot be predicted with this simple closed form estimation method, but the overall estimation is in good agreement with an assumption of the radiation resistance value R_{rad}=70Ω.
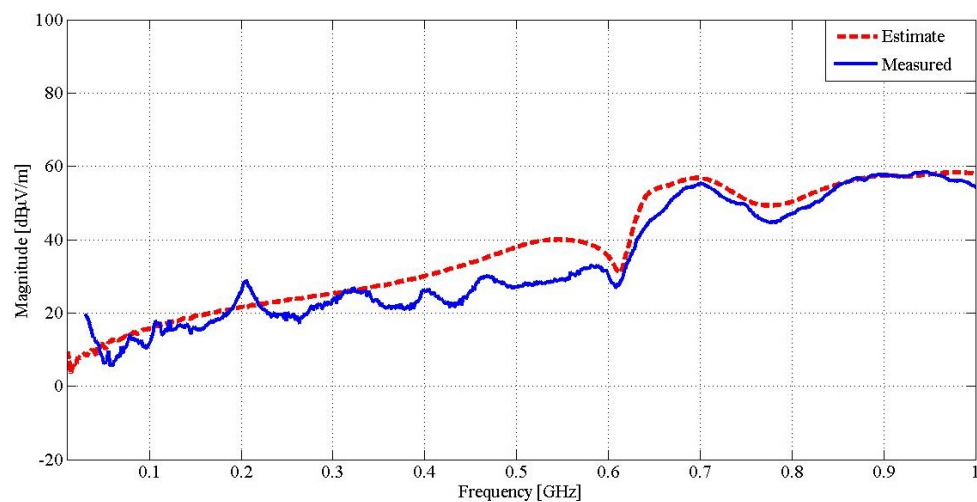

Figure 4.36. Measured and estimated field strength with HDMI cable

5. CONCLUSION AND FUTURE WORK

A systematic methodology to quantify the EMI coupling within a DVI system has been studied and validated. The systematic approach refers to breaking down of the DVI signal link into different blocks and quantifying the effect of each block towards the EMI performance of the system. Understanding the coupling paths within the system provides a better insight into debugging the EMI issues. Based on the coupling path study a transfer function was derived which determines the AM current on the DVI cable for a given DM input power and using simple field calculations we determine the emission level at the operating DVI clock frequencies. It also allows in identifying and quantifying the different imperfections on the DVI connector shell and connectorcable assembly structures so as to determine the most important slot/gap. Thus helping in identifying the dominating source through which the internal CM currents can leak out as AM currents.

The major advantage of this is to be able to quickly estimate the radiated fields for checking the EMI performance of the system. In this process a test setup was designed which can be used for screening of different cables based on their shielding performance. The same setup can be extended to other cable-connector systems as well, such as, HDMI, USB, etc. Making design modifications on the connector body/different interfaces and observe its impact in the radiated fields without heavy dependency on computational resources saves both time and effort. The disadvantage is that this method can predict an approximate solution only for the strong DVI harmonics. The other frequency bands in the system can be dominated by other noise sources in the system thus rendering this TF based approach ineffective. Based on this study the design suggestions which can be strongly supported to reduce EMI problems in this system are; (i) Designing a better contact between the DVI connector

shell and body frame, and (ii) Ensuring a better metal connection at the interface of the DVI connector shell and DVI cable mating shell.

BIBLIOGRAPHY

[1] Digital Display Working Group. Digital visual interface dvi. Technical report, Digital Display Working Group, April 1999.

[2] B. Archambeault, S. Connor, M.S. Halligan, J.L. Drewniak, and A.E. Ruehli. Electromagnetic radiation resulting from pcb/high-density connector interfaces. *IEEE Transactions on Electromagnetic Compatibility*, 55:614–623, 2013.

[3] H.W. Ott. *Noise Reduction Techniques in Electronic Systems*. Wiley, 1976.

[4] D.M. Hockanson, J.L. Drewniak, T.H. Hubing, T.P. Van Doren, Fei Sha, and M.J. Wilhelm. Investigation of fundamental emi source mechanisms driving common-mode radiation from printed circuit boards with attached cables. *Electromagnetic Compatibility, IEEE Transactions on*, 38(4):557–566, Nov 1996.

[5] Clayton R. Paul. A comparison of the contributions of common-mode and differential-mode currents in radiated emissions. *Electromagnetic Compatibility, IEEE Transactions on*, 31(2):189–193, May 1989.

[6] Constantine A. Balanis. *Antenna Theory: Analysis and Design*. Wiley, 2005.

[7] K.F. Casey and E.F. Vance. Emp coupling through cable shields. *IEEE Transactions on Electromagnetic Compatibility*, pages 100–106, 1978.

[8] Thomas Kley. Measuring the coupling parameters of shielded cables. *IEEE Transactions on Electromagnetic Compatibility*, 35:10–20, 1993.

[9] R. Tiedemann and K.-H. Gonschorek. Simple method for the determination of the complex cable transfer impedance. In *Electromagnetic Compatibility, 1998. 1998 IEEE International Symposium on*, volume 1, pages 100–105 vol.1, Aug 1998.

[10] S. Radu, Y. Ji, J. Nuebel, J.L. Drewniak, T.P. Van Doren, and T.H. Hubing. Identifying an emi source and coupling path in a computer system with sub-module testing. In *Electromagnetic Compatibility, 1997. IEEE 1997 International Symposium on*, pages 165–170, Aug 1997.

[11] W. Graf and E.F. Vance. Shielding effectiveness and electromagnetic protection. *IEEE Transactions on Electromagnetic Compatibility*, 30:289–293, 1988.

[12] Daryl Gerke and Bill Kimmel. Emi and emissions: rules,regulations, and options. *EDN Designers Guide to Electromagnetic Compatibility*, 2001.

[13] A.B. Clewes. Rfi/emc shielding in cable connector assemblies. *Electronics and Power*, 33(11.12):741–744, November 1987.

[14] Intel. Emi design guidelines for usb components. Technical report, Intel, February 1999.

[15] L.K. Warne and K.C. Chen. Slot apertures having depth and losses described by local transmission line theory. *Electromagnetic Compatibility, IEEE Transactions on*, 32(3):185–196, Aug 1990.

[16] R.G. Kaires. The correlation between common mode currents and radiated emissions. In *Electromagnetic Compatibility, 2000. IEEE International Symposium on*, volume 1, pages 141–146 vol.1, 2000.

[17] Zhang Hong-xin, Lu Ying-hua, Che Shu-Liang, and Han Yu-nan. A study on the electromagnetic leakage arising from braided shielding cable. In *Radio Science Conference, 2004. Proceedings. 2004 Asia-Pacific*, pages 519–522, Aug 2004.

[18] D.M. Pozar. *Microwave Engineering*. John Wiley and Sons, 2010.

[19] J.L. Drewniak, Fei Sha, T.P. Van Doren, T.H. Hubing, and J. Shaw. Diagnosing and modeling common-mode radiation from printed circuit boards with attached cables. In *Electromagnetic Compatibility, 1995. Symposium Record., 1995 IEEE International Symposium on*, pages 465–470, Aug 1995.

VITA

Abhishek Patnaik earned his Bachelors degree in Electrical Engineering from Institute of Technical Education and Research, India in 2010. After completion of his bachelors, he worked as a Systems Engineer at Tata Consultancy Services, Kolkata, India for 1 Year(till July 2011). He has been a graduate student in the Electrical Engineering Department at Missouri University of Science and Technology since August 2011 and worked as a Graduate Research assistant under Dr. David Pommerenke from March 2012 to May 2015. He completed his Masters in Electrical Engineering at Missouri University of Science and Technology in May 2015.